

MOTION OF A HELICAL SPRING DUE TO DYNAMIC LOADING

by

David W. McDougall and Enzo O. Macagno

**Conducted as Part of the
Research Study of the Hydrodynamics of
Recoil Systems
Sponsored by
U.S. Army Rock Island Arsenal
Contract No. DA-11-070-508-ORD-988**

**Each transmittal of this document outside
the Department of Defense must have prior
approval of the R. & E. Division,
Rock Island Arsenal.**

**IIHR Report No. 112
Iowa Institute of Hydraulic Research
The University of Iowa
Iowa City, Iowa**

September 1968

TABLE OF CONTENTS

	<u>Page No.</u>
I. MOTION OF A HELICAL SPRING	1
Introduction	1
II. MATHEMATICAL MODEL	3
Classical theory of spring oscillations	3
Simplified, discrete-element model of the spring	6
III. COMPARISON OF RESULTS FROM THE MATHEMATICAL AND PHYSICAL MODELS	14
Experiments	14
Comparison of the results	16
Conclusions	18
IV. COMPUTATIONAL TECHNIQUE	25
Solution by the method of characteristics	25
Summary of wave-equation formulas	27
Computational scheme	29
Rigid-body motion	30
Rigid region attached to moving end	31
Rigid region attached to fixed end	34
Rigid region floating freely	34
Spring fully compressed	38
V. APPENDIX	39
Main Program - Spring Experiment	39
Subroutine Spring	41
Subroutine CONTRL	42
Subroutine MOVRIG	44
Subroutine MIDRIG	45
Subroutine FIXRIG	48
FORTRAN listing of computer programs	48

Motion of a Helical Spring
Due to Dynamic Loading

Introduction

As a part of a continuing study at the Iowa Institute of Hydraulic Research on the hydrodynamics of recoil mechanisms, an analysis of the recoil phase of the M140 Recoil Mechanism has been undertaken. Hydrodynamically, this mechanism is similar to the XM37 used as a basis for previous studies, but is perhaps, somewhat simpler in this respect. Mechanically, however, a complication has been introduced by the adoption of a coil spring to replace the nitrogen chamber used in the XM37 to provide a counter-recoil force. Of course, the spring acts also during the recoil phase, one of its ends remaining fixed while the other is rapidly accelerated and decelerated.

A study of the spring dynamics has been undertaken to determine its exact influence among the various retarding forces acting on the mechanism during the recoil cycle. For this purpose, the spring was treated as a deformable continuum in a manner similar to that already applied in the analysis of pressure waves in the hydraulic fluid of the recoil mechanism. Few restrictions were put on the internal motion of the spring elements; they may take any nonuniform spacing, and a number of them may become packed together acting temporarily as a solid mass. In regard to the analysis of the complete mechanism, a nonuniform distribution of the coils of the spring must result in external forces exerted by the spring that are different from those applied by a supposedly static spring. This should be of special importance if the time of propagation of a wave through the spring and the time of recoil are of the same order of magnitude. The method described in this report for the analysis of the coil spring can be used for any spring of helical shape with a moving end and a fixed end. The latter restriction, however, could be removed without any particular difficulty.

The incorporation of the force generated by the spring (considered as a dynamic element of the system) into the analysis of the recoil mechanism has been completed, and the results will be summarized in the final report of this project. It is considered that this will provide a more accurate means of calculation, and will confine the remaining unknowns of the

problem to the hydrodynamics of the flow through control sections and to the relative motion between the hydraulic fluid and the moving parts such as the spring. At this point, a recommendation seems in order. For accuracy in computational modeling of the recoil mechanisms, as simple a geometry as possible, and location of the spring outside the hydraulic-fluid chamber seem highly desirable. With the computational techniques now available, calculation of the unsteady viscous flow during the recoil phase appears feasible if no internal spring is present. In fact, at the Iowa Institute of Hydraulic Research, problems involving accelerated viscous flows confined by simple two-dimensional geometries have already been solved numerically. But predicting the behavior of flow relative to any kind of spring would be, at the present time, only feasible when simplifying approximations of the drag and added-mass effect are made.

MATHEMATICAL MODEL

1. Classical theory of spring oscillations.

The deflection of axially loaded helical springs can be calculated by assuming that their elements behave as bars under torsion. The well-known expression for the deflection:

$$\xi = \frac{8PD^3n}{Gd^4} \quad (1)$$

is thus obtained. Herein P is the load; D , the mean coil diameter; d , the bar diameter; G , the shear modulus of elasticity; n , the number of active coils. For a given spring, this formula, which is reportedly quite accurate (1), can be expressed simply as

$$\xi = \frac{P}{K} \quad (2)$$

where K is the elastic constant of the spring.

Because of the important functions performed by springs in many machines, a theory of spring oscillations was developed many years ago. The essential steps for the derivation of the basic differential equation for springs undergoing oscillations of small amplitude will be reviewed here because it is helpful to refer to the governing differential equation before constructing a discrete-element model of the spring.

Consider an element of the spring bar of length ds (Fig. 1) located at a distance s measured along the helical axis of the bar.

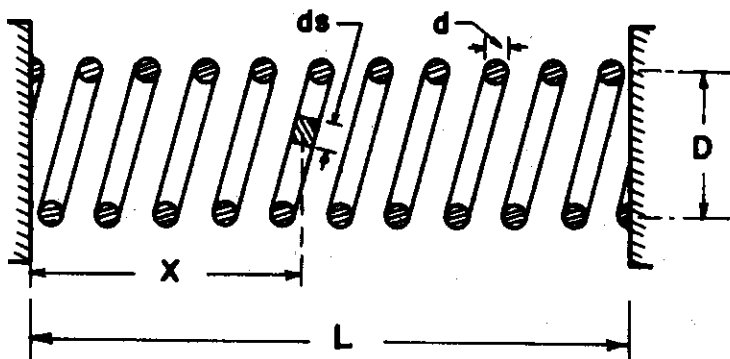


Figure 1

(1) Wahl, A. M., "Further Research on Helical Springs of Round and Square Wire," *Trans. ASME*, v. 52, 1930.

The location of the element, when the spring is in equilibrium, is given by X , which is measured along the linear axis of the spring. When the spring oscillates, the element will be at a distance indicated by x . The mass of the element is $(1/4)\rho d^2 ds$, where ρ is the specific mass (mass/volume). The acceleration of the element is given by $\partial^2 x / \partial t^2$. The net elastic force acting on the element is

$$\frac{\partial F}{\partial s} ds = \frac{\pi G d^4}{8 D^2} \frac{\partial^2 x}{\partial s^2} ds \quad (3)$$

which results from expressing F , the spring force, in terms of the local deflection (2).

If resistance to motion is neglected, the equation of motion reduces to

$$\frac{\pi d^2}{4} \rho \frac{\partial^2 x}{\partial t^2} = \frac{\pi G d^4}{8 D^2} \frac{\partial^2 x}{\partial s^2} \quad (4)$$

or to its equivalent:

$$\frac{\partial^2 x}{\partial t^2} = c^2 \frac{\partial^2 x}{\partial X^2} \quad (5)$$

in which X has been used instead of s , taking into account that $s = \pi D n X / L$, and in which

$$c = \frac{L d}{\sqrt{2} \pi D^2 n} \sqrt{\frac{G}{\rho}} \quad (6a)$$

A more convenient form of the parameter c is

$$c = L \sqrt{\frac{K}{m}} = \sqrt{\frac{K L}{\sigma}} = \frac{\sqrt{K m}}{\sigma} \quad (6b)$$

Herein, m is the mass of the spring, and σ is the mass per unit length in the X direction. σ may also be called the linear density of the spring. Because ρ will not be used in the following development, σ will be designated more simply as the density. Eq. (5) is the well-known one-dimensional

(2) Wahl, A. M., *Mechanical Springs*, 2nd ed., p. 287, McGraw-Hill, New York, 1963.

wave equation, and applies also to transverse oscillations of springs, longitudinal vibration of uniform bars, pressure waves in liquid-carrying conduits, and to certain types of waves in open channels. It was the analogy with the water-hammer phenomenon which first suggested to the authors the possibility of studying transient vibrations of a spring by means of methods used in hydraulic engineering for transient phenomena in pipelines. Further study of transients in springs led to the realization that the analogy with waves in a conduit running partially full is also useful, especially when coils of the spring consolidate. This occurrence may be likened to surges of sufficient height within the conduit to cause portions of it to run full.

The Eq. (5) can be integrated by the method of separation of variables. The result, in terms of circular functions, shows that the spring possesses an infinite number of possible natural frequencies of oscillation. Several of them can be excited simultaneously, producing a very complex motion. In the M40 recoil mechanism the spring is initially at rest before being subjected to an acceleration and a deceleration of very short durations. It appears plausible to assume that the motion is best described by the initial propagation of a simple wave from the moving end, upon which, after a time of the order L/c , a reflected wave is superimposed. At most, a second reflection may occur. In this respect, the spring behavior is very similar to water hammer transients for which very reliable methods are available. Such methods were applied to the analysis of the transients in the hydraulic fluid in the XM37 recoil mechanism, (3, 4).

Obtaining classical solutions of Eq. (5) in terms of Fourier expansions does not appear impossible to the authors. However, this approach would become very difficult in cases where coils consolidate and form temporarily solid portions. For example, detecting the condition of incipient consolidations would appear to be much more difficult by classical, analytical methods than by electronic computer.

If one plots x versus X for different times, it is easy to recognize that for a certain value of $dx/dX = \epsilon_0$, the indication would be

(3) Macagno, E. O., and Macagno, M., "Pressure-Wave Analysis for Variable Length of a Fluid Column," *Ninth Congress IAHR*, Dubrovnik, 1961.

(4) Macagno, E. O., "Pressure-Wave Analysis," *IIHR Report to the Rock Island Arsenal*, Contract No. DA-11-670-508-ORD-988, January, 1963.

This behavior will also be prescribed for the model in the cases in which a compression force F is applied to any of its parts; the density may not exceed σ_m either at any point, or in any element. In the spring, the consolidation of coils is equivalent to the insertion of an inelastic segment in the cylinder in the mathematical model. One could consider that the solid portion can still transmit elastic waves back and forth, but at a much greater celerity than the celerity along the free-coil portions. Consequently, the assumption has been made that when coils consolidate, the corresponding portions of the spring and the model can be treated as a rigid body of variable length, temporarily inserted in the spring. The length of the rigid portion is a function of time. It may form, grow, decrease, and eventually disappear during the recoil motion.

It may be useful to compare the model to a number of bellows connected in series but with inner rigid elements which limit the compression of each. Whether or not the interpretation of the mathematical model as a series of bellows is appropriate, the important principle is that the mathematical model must simulate the essential features of the prototype with satisfactory fidelity.

If we call F the compression force, we have for a statically loaded spring

$$F = K\xi \quad (8)$$

as the constitutive equation, valid for $\xi \leq \xi_m$. The maximum value of the density σ is then given by

$$\sigma_m = \frac{m}{L_0 - \xi_m} \quad (9)$$

where L_0 is the initial length of the spring.

The principle of mass conservation, which must apply both to a statically loaded spring and to the model, may be written

$$m = \sigma_0 L_0 = \sigma L = \text{const} \quad (10)$$

Likewise, for any of the elements of the moving spring or the model,

$$\sigma \Delta x = \text{const} \quad (11)$$

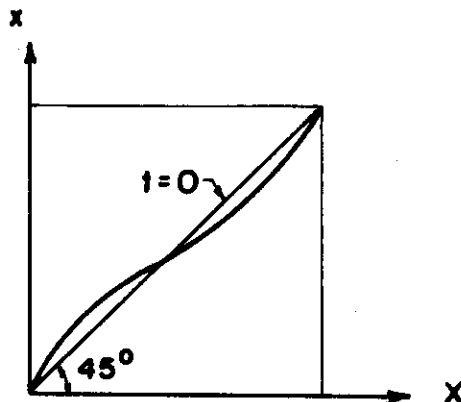


Figure 2

that consolidation has occurred or is imminent. Once it has occurred, the spring must be subdivided, and if it occurs somewhere in the middle, analysis along classical lines appears to be very difficult.

2. Simplified, discrete-element model of the spring.

In the analysis of the water-hammer rapid transients, the basic approach to the solution is represented by D'Alembert's rather than Lagrange's form of the general solution of Eq. (4), (or its equivalents), i.e. by

$$x = \phi(X + ct) + \psi(X - ct) \tag{7}$$

Only when steady oscillatory phenomena are considered, is the other form usually preferred. Eq. (7) enables direct access to the graphical and numerical methods applied in previous reports on the hydraulic aspects of the recoil phase of the XM37 mechanism, (3). The procedure to be followed is described in the literature on water hammer as the method of characteristics. The one-dimensional continuum for which the wave-propagation phenomena are investigated is divided into segments, elementary waves are allowed to propagate through segments of such lengths that they meet at the interfaces of the elements, and the superposition as well as the reflection and transmission of resulting waves is determined.

The mathematical model of the spring is constructed by representing it by a cylinder of uniform cross section made of elastic material, that behaves like a spring under static loading i.e. according to Eq. (2). As in the case of the actual spring, the deflection of the model will be limited by a value ξ_m , at which the spring becomes rigid and the density becomes σ_m .

from which

$$\Delta x d\sigma + \sigma d(\Delta x) = 0 \tag{12}$$

If we apply the compression force dF to the element of length δx , we have

$$dF = KL \frac{d(\Delta x)}{\Delta x} \tag{13}$$

which results from applying Eq. (8) to evaluate the effect of dF on the length L , and from assuming that the deflection for the length δx must be $\delta x/L$ times less.

From (12), (13) and (6b), we obtain

$$\frac{dF}{d\sigma} = \frac{KL}{\sigma} = c^2 \tag{14}$$

This expression can also be obtained from an analysis of the propagation of an infinitesimal wave, (Fig. 2). The wave front travels at a

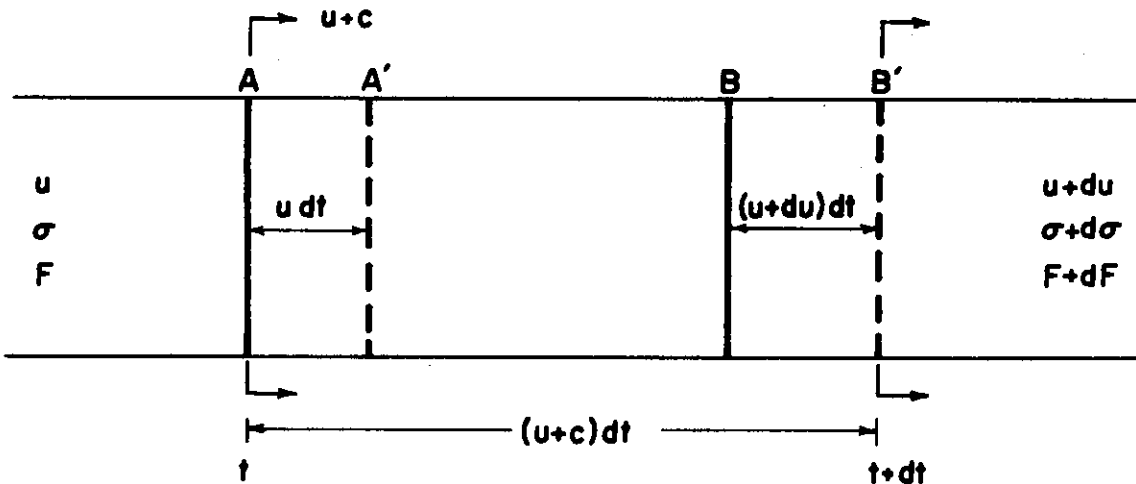


Figure 3

speed c with respect to the medium. The state to the left of the front is represented by velocity u , density σ , and spring force F , while at the right, the values are $u + du$, $\sigma + d\sigma$, and $F + dF$. As the wave front travels, changes occur locally; $u + du$, $\sigma + d\sigma$, $F + dF$ become u , σ , F respectively. In Fig. 2, an element AB is shown at the time t and then in the position $A'B'$ at the time $t + dt$. The derivation will thus be based on a Lagrangian approach consistent with the treatment of the mathematical model of the spring, which also is based on a consideration of a number of elements and on following their motion and their changes in length, density,

and spring force.

From conservation of mass, the mass is the same for the element at AB and at A'B', i.e.

$$\sigma(c - du)dt = (\sigma + d\sigma)c dt$$

from which

$$-\sigma du = c d\sigma \quad (15)$$

During the time interval Δt , the mass of the element has been under the action of the impulse $-dFdt$, and its velocity has changed from u to $u + du$.

Application of the impulse-momentum relationship gives

$$dFdt = (\sigma + d\sigma)c dt du = \sigma \left(1 + \frac{d\sigma}{\sigma}\right) c du$$

from which

$$dF = -\sigma c du \quad (16)$$

if $d\sigma/\sigma$ is much smaller than unity (which is precisely what is assumed in treating an infinitesimal wave). From (15) and (16),

$$\frac{dF}{d\sigma} = c^2 \quad (17)$$

is obtained.

Since the model is a continuum, and behaves essentially as a one-dimensional "flow", it is reasonable to apply the equations of continuity and the first of the Euler equations to obtain

$$\frac{\partial \sigma}{\partial t} + u \frac{\partial \sigma}{\partial X} + \sigma \frac{\partial u}{\partial X} = 0 \quad (18)$$

$$\sigma \left(\frac{\partial u}{\partial t} + u \frac{\partial u}{\partial X} \right) + \frac{\partial F}{\partial X} = 0 \quad (19)$$

The classic equations for fluid flow coincide with the two preceding equations if analogies between volumetric mass density ρ and the linear mass density σ , and between the pressure p and the elastic force F are established. In fact, one system of equations can be derived from the other by the simple device of multiplying the classic form of the equations by the constant cross-sectional area A of the model representing the spring.

In our model, $\sigma = \sigma(F) = \sigma[F(x,t)]$. Hence,

$$\frac{\partial \sigma}{\partial X} = \frac{d\sigma}{dF} \frac{\partial F}{\partial t} = \frac{1}{c^2} \frac{\partial F}{\partial t} \quad (20)$$

$$\frac{\partial \sigma}{\partial t} = \frac{d\sigma}{dF} \frac{\partial F}{\partial t} = \frac{1}{c^2} \frac{\partial F}{\partial t} \quad (21)$$

From Eqs. (18), (20), and (21), the following is obtained:

$$u \frac{\partial F}{\partial X} + \frac{\partial F}{\partial t} + \sigma c^2 \frac{\partial u}{\partial X} = 0 \quad (22)$$

It can easily be verified that the product σc is constant. Therefore the new dependent variable

$$f = \frac{F}{\sigma c} \quad (23)$$

can be introduced, thus transforming Eq. (22) into

$$L_1 = u \frac{\partial f}{\partial X} + \frac{\partial f}{\partial t} + c \frac{\partial u}{\partial X} = 0 \quad (24)$$

In terms of the variable f , equation (19) becomes

$$L_2 = u \frac{\partial u}{\partial X} + \frac{\partial u}{\partial t} + c \frac{\partial f}{\partial X} = 0 \quad (25)$$

The two equations (24) and (25) will now be combined linearly, in the form $L_1 + \lambda L_2 = 0$, and values of λ will be established taking into account the total derivatives:

$$\frac{du}{dt} = \frac{\partial u}{\partial X} \frac{dX}{dt} + \frac{\partial u}{\partial t} \quad (26)$$

$$\frac{df}{dt} = \frac{\partial f}{\partial X} \frac{dX}{dt} + \frac{\partial f}{\partial t} \quad (26a)$$

The above-mentioned linear combination yields

$$(\lambda c + u) \frac{\partial f}{\partial X} + \frac{\partial f}{\partial t} + \lambda \left[\left(\frac{c}{\lambda} + u \right) \frac{\partial u}{\partial X} + \frac{\partial u}{\partial t} \right] = 0 \quad (27)$$

If the conditions

$$\frac{dX}{dt} = \lambda c + u \quad ; \quad \frac{dX}{dt} = \frac{c}{\lambda} + u$$

are required, the multiplier λ becomes determined by

$$\lambda c = \frac{c}{\lambda}$$

It can easily be seen that $\lambda = \pm 1$. The system of equations (24) and (25) can now be replaced by the following system:

$$c^+, \left\{ \begin{array}{l} \frac{df}{dt} + \frac{du}{dt} = 0 \\ \frac{dX}{dt} = c + u \end{array} \right. \quad (28)$$

$$c^-, \left\{ \begin{array}{l} \frac{df}{dX} - \frac{du}{dt} = 0 \\ \frac{dX}{df} = -c + u \end{array} \right. \quad (29)$$

The second equation in each pair defines a direction of the corresponding path or characteristic line in the X-t plane. If we observe the motion along the characteristics from a moving element of our model, the inclinations of the characteristics become $\pm c$. To this we must add that the time of travel through the element (or half of it) becomes independent of the actual length of the element. In fact, the time to traverse an element of length Δx with velocity c is $\Delta x/c = \sigma_0 \delta x_0 / \sigma c$, which is the ratio of two constant quantities. This makes the calculations much simpler because a constant time increment can be introduced in the discrete formulation of the Eqs. (28) and (29). One then obtains

$$f_P - f_A + u_P - u_A = 0 \quad (30)$$

$$x_P - x_A = c\Delta t$$

$$f_P - x_B - (u_P - U_A) = 0 \quad (31)$$

$$x_P - x_B = -c\Delta t$$

which are written for two points A, B (see Fig. 3) for which the values of u and f are known, and for a point P for which they are desired. The point P is at the center of an element, and A, B are at the centers of the

two neighboring elements.

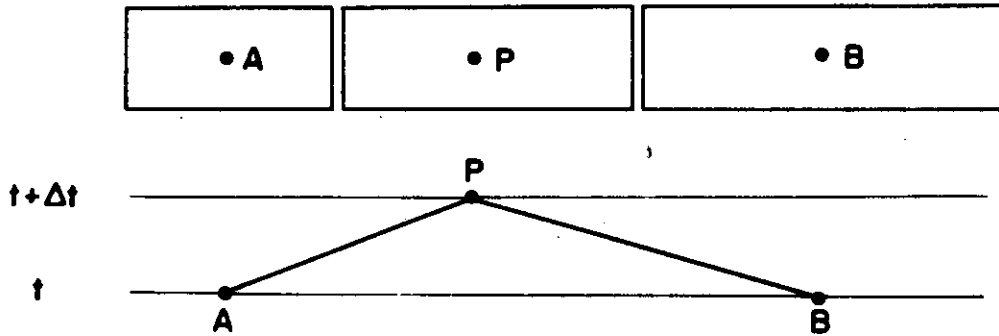


Figure 4

By solving the system of equations C^+ and C^- new values of u and f are determined. Once u and f are known, one can predict the new positions of the elements, their new lengths and corresponding densities, and also the force F . As long as the length of any of the elements does not become less than the minimum, or the density does not exceed the maximum, the coils are assumed to remain free. If, at a certain time t , a group of elements appear compressed beyond the established limit, the procedure must be supplemented to accommodate a rigid portion either at the middle of the spring or at one of the two ends.

In figure 5, the results of several steps of a hypothetical calculation

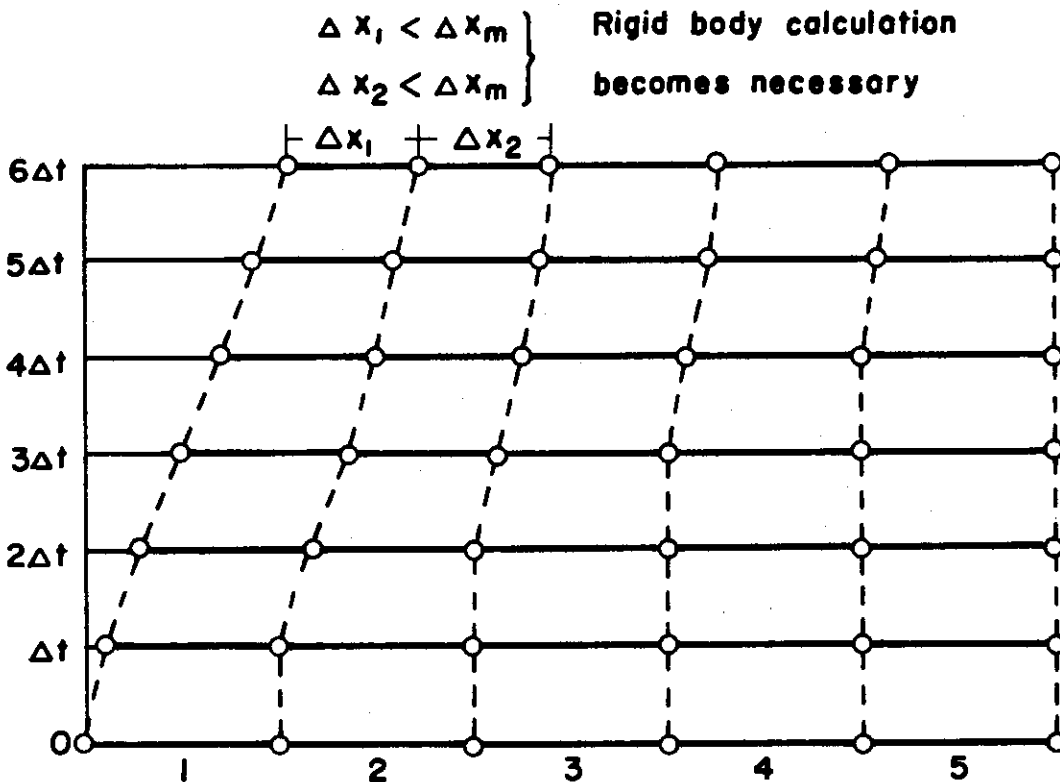


Figure 5

are depicted, in a qualitative manner, for a small number of elements. The moving end is at the left, and the fixed end at the right. After six steps, two elements appear shorter than the minimum admissible Δx . At this point it becomes necessary to re-examine the motion of these elements and of their immediate neighbors by using a combination of the wave equation (or its equivalents (30) and (31)) and the equation for rigid-body motion. The computational procedure for rigid portions at the moving end, in the middle, and at the fixed ends are given in detail in the chapter entitled Computational Technique; we indicate here only the basic considerations related to the formation of a rigid portion in the middle of the spring.

Suppose that the lengths of the elements i to $i+n$ become less than Δx_m at the time $t+\Delta t$. The motion of a portion of the spring between the section $i-1$ to $i+n+1$ must then be recalculated assuming that at an intermediate time between t and $t+\Delta t$ it became rigid. This is caused by an impulse due to the force F_{i-1} from the left side and the force F_{i+n+1} from the right side which act during the time interval $t, t+\Delta t$. The momentum change must be expressed in terms of the common velocity V_{rig} of the elements which form the rigid portion, the velocities of the elements which are elastic at the time t (indicated by the superscript j) and those which remain elastic at $t+\Delta t$ (indicated by the superscript $j+1$). The latter are the two elements at the ends, i.e. $i-1$ and $i+n+1$. The impulse-momentum relationship is then as follows:

$$(F_{i-1} - F_{i+n+1})\Delta t = \frac{\Delta m}{2}(u_{i-1}^j + u_{i+n+1}^j) + \Delta m \sum_{j=i}^{i+n} u_j^t - \frac{\Delta m}{2}(u_{i-1}^{j+1} + u_{i+n+1}^{j+1}) + n\Delta m V_{rig} \quad (32)$$

From this expression, V_{rig} can be obtained; u_{i-1}^{j+1} and u_{i+n+1}^{j+1} can be determined using the characteristics method. It may be necessary to readjust the calculation in order to decide if the rigid portion is not actually somewhat longer. Once this is done, everything is ready for the next step.

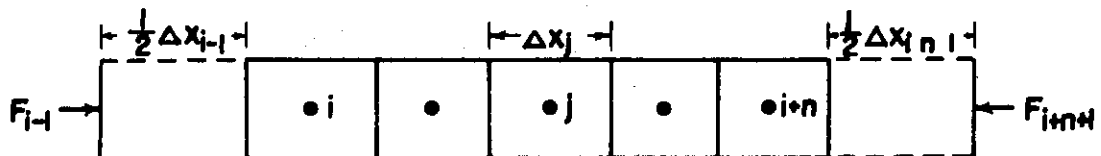


Figure 6

COMPARISON OF RESULTS FROM THE MATHEMATICAL AND PHYSICAL MODELS

Experiments

A series of experiments with a helical steel spring was performed at the Rock Island Arsenal under the supervision of Mr. Robert Coberly. In the planning of these experiments, previous results obtained from the mathematical model developed at the Iowa Institute of Hydraulic Research were taken into account. It was possible for the analysts at the Institute to indicate to the experimenters at the Arsenal the conditions which should be established in order to obtain different cases of internal motion of the spring. To provide an experimental check of calculated motions, some cases in which no coil contact would occur were considered of basic importance. Should the mathematical model fail to reproduce the less severe cases, there would be no point in comparing the models for more severe conditions, except perhaps for an indication of relative values of discrepancy.

The characteristics of the spring used in the experiments are given in Table 1.

TABLE 1

Diameter of spring	D = 5.72 in.
Diameter of rod	d = 0.375 in.
Total weight of spring	6.28 lb.
Active weight	5.86 lb.
Elastic constant	15.0 lb./in.
Total height of unloaded spring	17.6 in.
Active height	17.225 in.
Minimum height (maximum compression)	3.80 in.
Number of coils	11 and 5/8
Number of active coils	10 and 3/8

The determination of the number of active coils was based on current practice for helical springs. Wahl (2) suggests a value of 1/4 coil more than the

(2)Wahl, A. M., *Mechanical Springs*, 2nd ed., pp. 65-66, McGraw-Hill, New York, 1963.

number of free coils as an acceptable compromise among the many recommendations found in the literature.

The spring was set up vertically around a metal cylinder. Contact between the spring and the cylinder should occur only if the spring buckles during the motion. Such contact would introduce friction forces which would locally affect the motion of the coils. The contact friction was considered to be negligible.

A variety of weights were available to be dropped on the spring from above. Each weight was axisymmetric with a hole along its axis of symmetry to accommodate the metal cylinder and to likewise be free to slide vertically with negligible contact friction. A wide range of drop heights could be selected as well.

The spring was instrumented with strain gauges because of the interest of the Arsenal engineers in the stresses. This added an unknown factor from the point of view of the analysts (who were concerned essentially with the motion of the spring) because each coil would entrain an electrical lead in its motion. It was made certain, however, that the strain gauges were mounted in such a way that they would not disturb the natural contact between coils. Because it was known that experiments would be of short duration, it was decided to take high-speed motion pictures of the motion of the coils. In addition to providing adequate illumination, thin white lines were painted on the edges of the coils to define as exactly as possible their position. Scales and an electric timer were included so that the position and the corresponding time would be registered in each frame of the film.

From several films taken during the experiments five were selected for data reduction at the University of Iowa. They were renumbered in the order of increasing complexity of internal motion and/or severity of dynamic loading. The magnitudes of the weight dropped on the spring and the heights above the spring from which they were released are included in the legends in each of figures 7 to 11, for Runs 1 to 5.

Data was obtained from the film record through the use of a model C-11D Vanguard Motion Analyzer with M-16CD Projection Head which was available at the University. Individual frames were enlarged and projected on a screen before the operator. The operator, by matching a horizontal hairline

with selected coils on the spring image, directly read scaled position data from a digital readout device. The scaled positions of reference points were obtained for subsequent data reduction. Time was obtained by visual observation of the clock image. Final data reduction, correcting the position data, was accomplished with the help of a simple digital-computer program, which is not sufficiently important to be listed here.

Comparison of the results

The spring constant, one of the essential characteristics of the spring, was determined at the University of Iowa. The curve of load-versus-deflection is not exactly linear, but the deviation from a straight line is relatively small. It was decided to proceed with the best linear fit to the curve of load-versus-deflection, and consider the introduction of a non-linear behavior only if the discrepancies between the two models should become unacceptable.

The computational model was then run with values of the parameters which would correspond as closely as possible to those of the experiments. The computational technique has been made the subject of an entire chapter, and the description of the computational experiment need not be repeated here.

The results of the computational model are shown by the four solid curves in each of the figures 7 to 11. On these figures the experimental points are indicated by circles.

In Run No. 1 there was no contact between coils in the physical model and, correspondingly, no rigid portions in the mathematical model. The displacement curve for the top element of the mathematical model and the experimental points for the top of the spring agree very well. The internal motion, which has been represented for coils 3, 5, and 8, shows good agreement for the first half of the run, during which the spring is being compressed (although internally it may be decompressing in its lower portion). In the second half of the run, when the weight reverses its motion, and the spring is undergoing a stretching with respect to the state of maximum shortening, some discrepancies appear, which seem to be characteristic of some time lag. In figure 7, one can easily identify the propagation of waves back and forth from the moving end to the fixed end. This is especially clear

if one inspects the results of the computational model. This shows that the curves are really made of segments which change, often rather abruptly, in direction as the wave front reaches the corresponding point along the spring. The experimental points are much less numerous than the calculated points, and by themselves were insufficient in number to depict the motion continuously. Therefore, the experimental curves (not traced in the drawings) should be envisioned taking into account the wave-propagation nature of the internal motion. This brings the computed and the experimental values into a little better agreement.

Runs Nos. 2 and 3 each exhibited rigid-body formation. Run No. 2 experienced only a small rigid region, formed and dispersed at the fixed end within a few milliseconds, beginning 0.160 sec. after the motion was initiated. Run No. 3 experienced more. The following highlights for Run No. 3 are described in chronological order:

1. A rigid region formed at the fixed end beginning at 0.096 sec., involving 24% of the spring, and was dispersed by 0.110 sec.
2. A rigid region formed at the moving end beginning at 0.126 sec., eventually involving 29% of the spring.
3. The above rigid region became detached at 0.134 sec. and this floating rigid region continued to exist until 0.139 sec.
4. Another rigid region formed at the fixed end beginning at 0.157 sec., involving 23% of the spring, and was dispersed by 0.170 sec.

Figures 8 and 9 for Runs 2 and 3 again show better agreement for the first phase than for the second. From the point of view of recoil and counter-recoil in a mechanism this is favorable, because the recoil phase is more important than the counter-recoil phase in the general design of recoil mechanisms.

Runs Nos. 4 and 5, as the corresponding figures 10 and 11 show, were such that the computational model became fully compressed. Nevertheless, some additional events occurred. In Run No. 4:

1. A rigid region formed at the fixed end beginning at 0.033 sec., involving 16% of the spring, and was

dispersed by 0.043 sec.

2. A rigid region formed at the moving end beginning at 0.064 sec., and grew until the entire spring became rigid at 0.075 sec.

In Run No. 5:

1. A rigid region formed at the moving end beginning at 0.065 sec., eventually involving 21% of the spring.
2. The rigid region became detached at 0.070 sec., and the floating rigid region continued to exist until 0.075 sec.
3. A rigid region formed at the fixed end beginning at 0.096 sec., and grew to involve 84% of the spring before shedding segments.
4. As the above rigid region continued to diminish in size, another rigid region formed at the moving end beginning at 0.110 sec. The latter experienced rapid growth and overtook the retreating front of the former. The entire spring became rigid at 0.112 sec.

The first phase is well predicted except at the very end. It was not considered necessary to run computations for the second phase. The experimental points show a rather regular behavior, and probably the mathematical model would have matched them nicely without, however, adding to the confidence in the model. The test of the case in which the spring starts from a fully compressed zero-velocity state and expands (being a case less severe than that of Run No. 1) was not considered to be worth including in the present comparison.

Conclusions

In conclusion, the comparison of experimental and calculated values shows, from the point of view of recoil mechanisms, a generally satisfactory agreement. The accuracy with which the motion is predicted for the displacements in the recoil phase is reasonably good. Improvements could come from taking into account the actual relation between force and deflection if it were found that all the springs used in recoil mechanism of a certain series exhibit the same non-linearity. An approximating curve could then be used

instead of an average value of the spring constant. Before engaging in this refinement, though, it would be advisable to develop another type of refinement of the mathematical model. If the spring in a recoil mechanism is located within a chamber containing hydraulic fluid, it becomes subject to forces derived from fluid moving relative to the coils. Therefore, added mass effects as well as fluid drag should be introduced into the mathematical model. Probably, these fluid effects are more important than the slightly non-linear relationship between force and deflection.

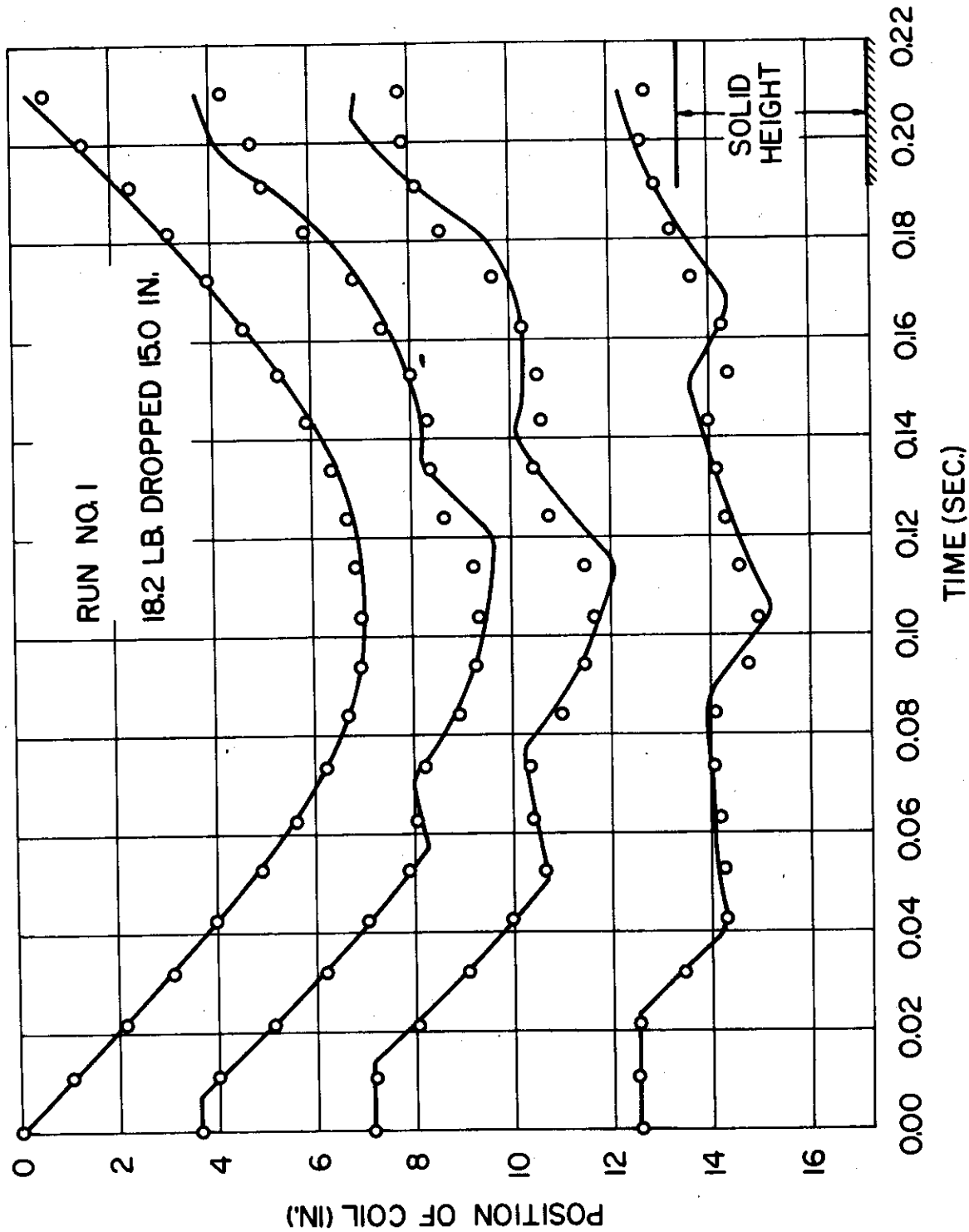


Fig. 7. Comparison of computational and physical models

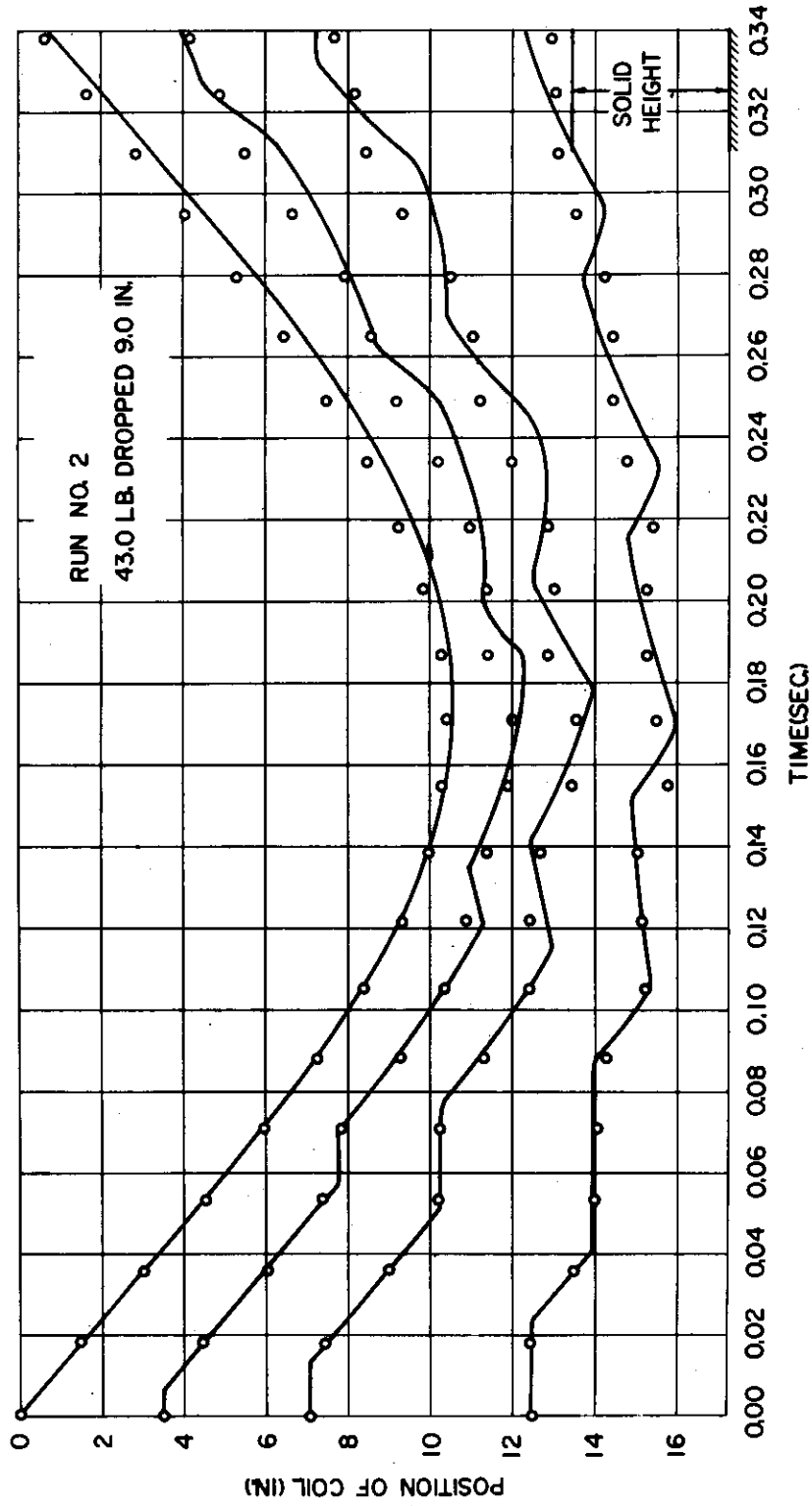


Fig. 8. Comparison of computational and physical models

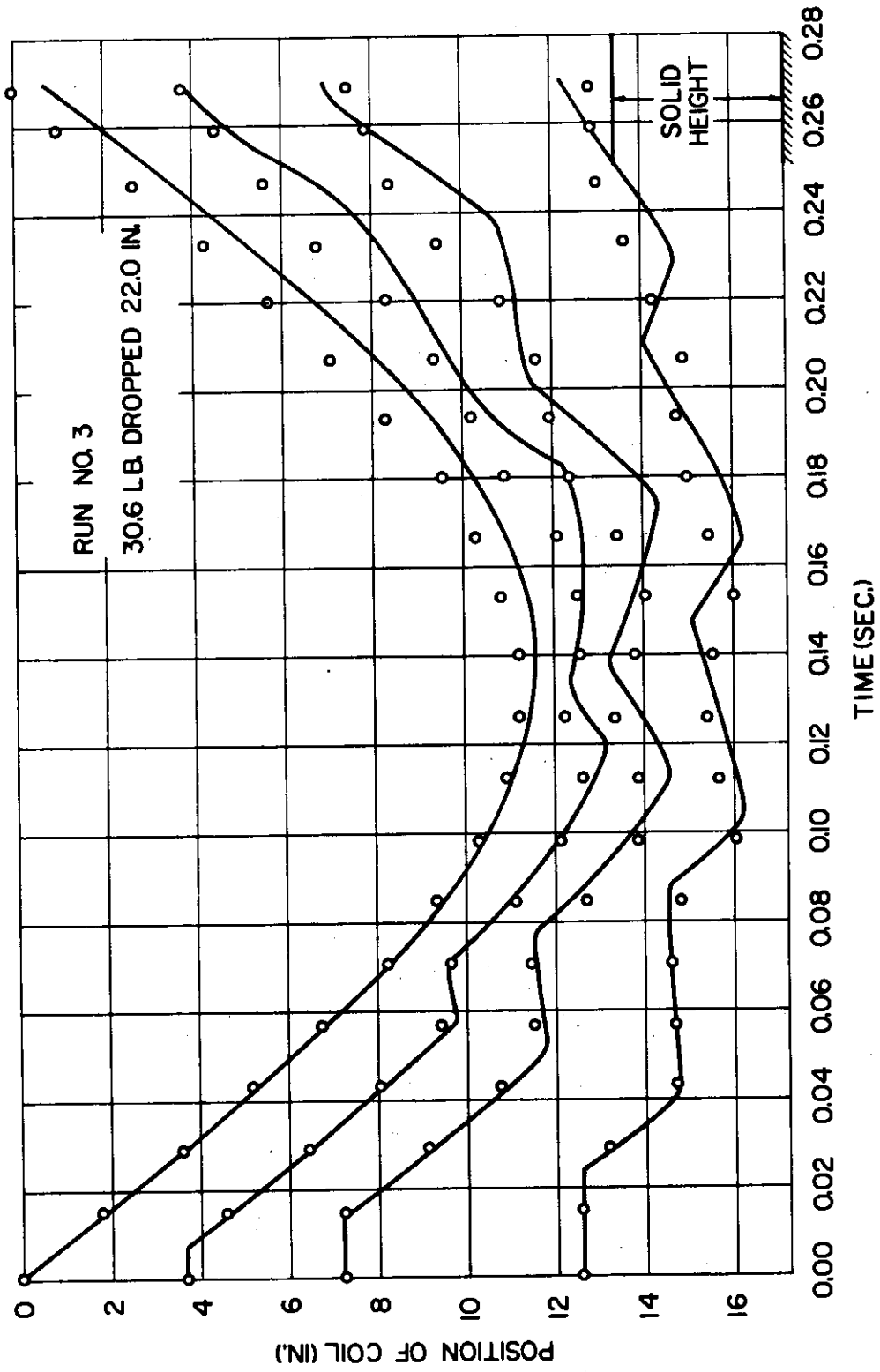


Fig. 9. Comparison of computational and physical models

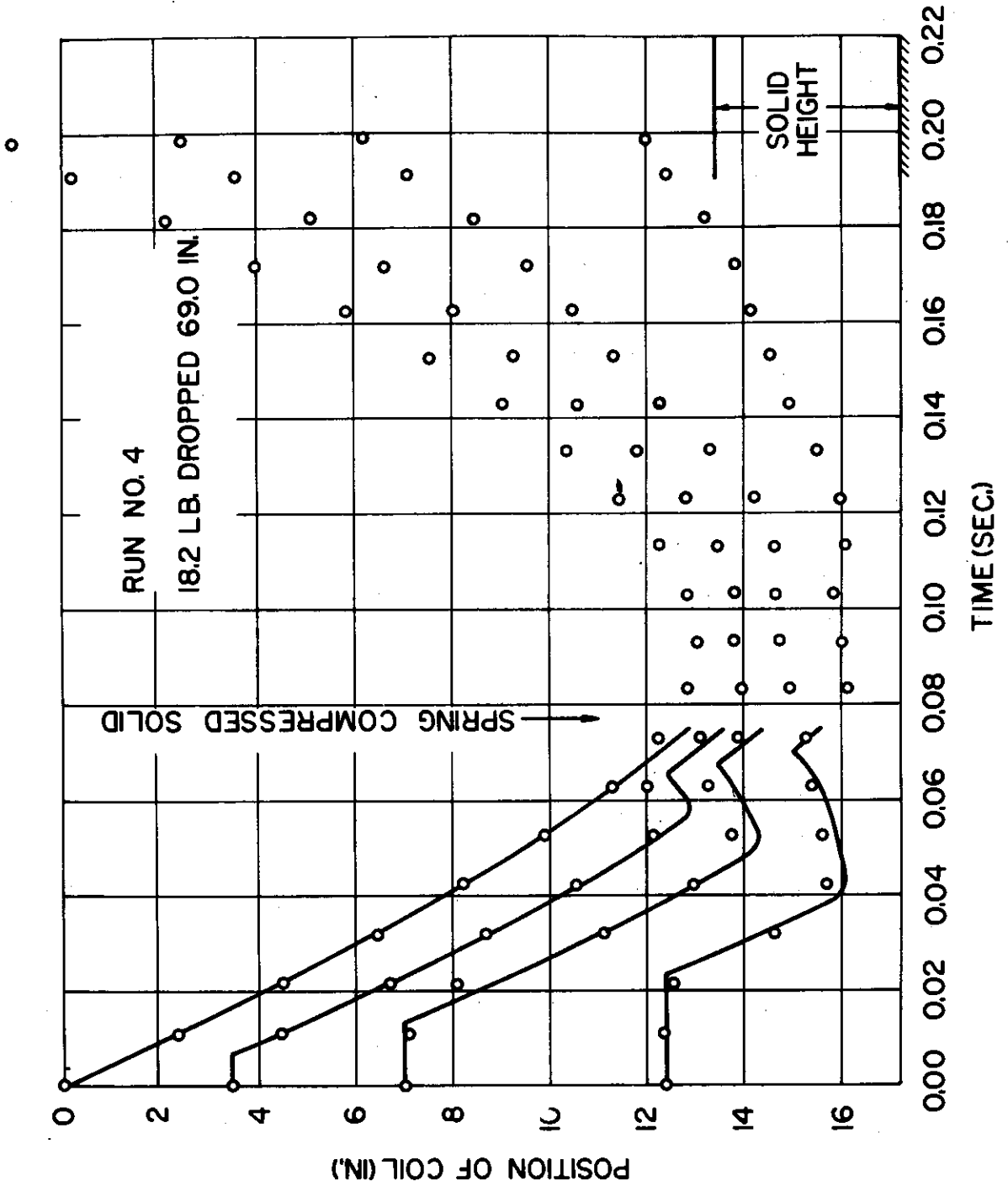


Fig. 10. Comparison of computational and physical models

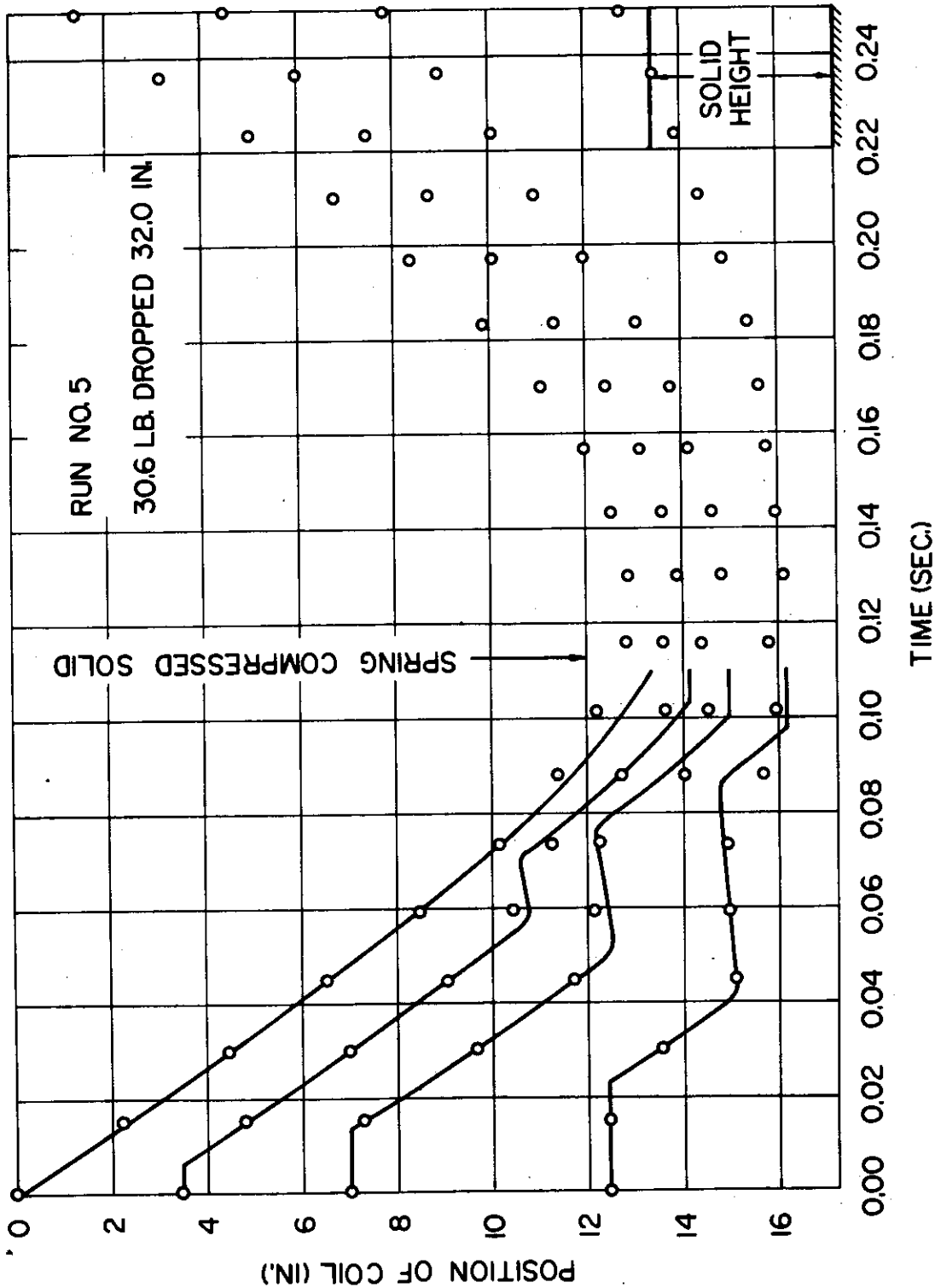


Fig. 11. Comparison of computational and physical models

COMPUTATIONAL TECHNIQUE

The one-dimensional model used in this analysis can be described as a series of elastic segments

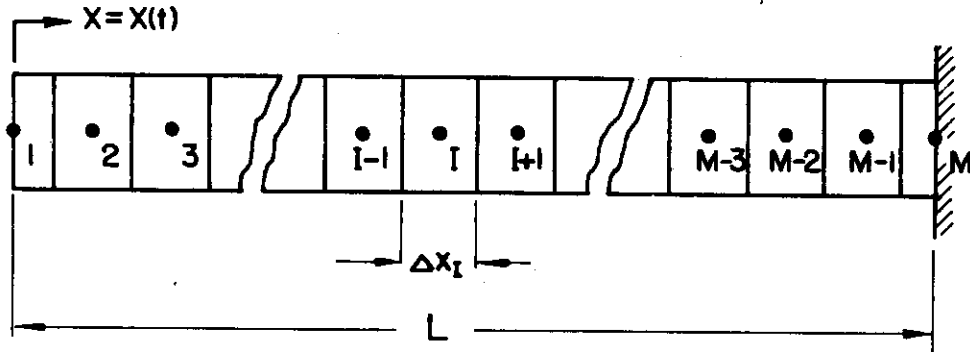


Figure 12

each numbered at its center, the point at which local behavior (e.g. velocity) and properties (e.g. density) are summarized. Both moving and fixed ends terminate with segments of one half the mass of the interior segments. This latter feature facilitates the application of boundary conditions.

A segment behaves elastically unless its density becomes too large (or, until Δx becomes too small), at which time the segment becomes rigid. This abrupt change in material behavior simulates the phenomenon of coil closure. The motion of segments influenced only by elastic forces is predicted by the wave equation, and the solution proceeds by the method of characteristics. When a segment becomes rigid, additional internal forces arise, and the solution proceeds with rigid-body-motion equations.

Solution by the method of characteristics

As discussed in chapter II, the sum and difference of the velocity, v , and the force function, $f = \int \frac{dF}{\sigma c}$, are constant along specified characteristic lines. The scheme is illustrated schematically in the following figure.

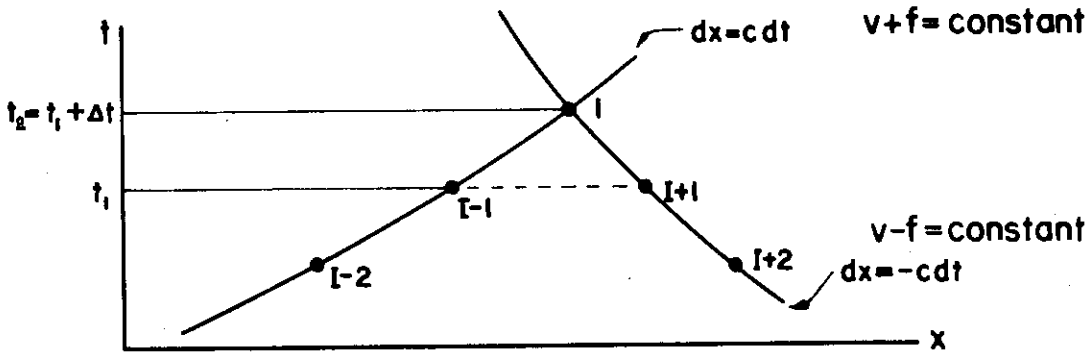


Figure 13

The characteristic lines are drawn as curves to illustrate the fact that the celerity, c , indeed varies with the density,

$$\sigma c = \sqrt{km} = \text{constant}. \quad (33)$$

However, because of this intimate link between celerity and density, a unique value of Δt can be found which causes the characteristic lines to pass through the exact center of neighboring segments as shown in the above figure. This property of the one-dimensional model comes as no surprise if one recalls the mechanism of wave propagation in the prototype. Torsion waves travel around the helical coil at a constant rate, and the length of the coil remains unchanged as the spring is flexed. Consequently, the travel time of an elementary wave, Δt , is associated with a unique length of the coil -- or segment size in the corresponding model.

The simplicity of computation offered by the above property suggests prescribing the M segments representing the spring as follows. Consider the spring in its unstretched form -- length L_0 and density σ_0 .

$$c = \frac{dx}{dt} = \frac{L_0 / (M-1)}{t} = \frac{\sqrt{km}}{\sigma_0} \quad (34)$$

Solve for $M-1$ and, in doing so, replace $\sigma_0 L_0$ by the mass, m .

$$M - 1 = \frac{\sqrt{m/k}}{\Delta t} \quad (35)$$

Perhaps at this point it is well to introduce FORTRAN notation in the formulas, which is the form of their ultimate use. The choice of variable

names should be evident by comparing with the above formula; SQRT is the FORTRAN-supplied square-root function.

$$M - 1 = \text{SQRT}(\text{MASS}/K)/\text{DELTA} + 0.5 \quad (36)$$

Inasmuch as an integer value for M is demanded, 0.5 has been added to achieve rounding off to the nearest integer rather than mere truncation.

The programmer has the option now of slightly readjusting any of the parameters MASS, K, or DELTA for the sake of agreement in his computations. For example, upon selecting the best value for M, K could be readjusted to be

$$K = \text{MASS}/((\text{FLOAT}(M-1) * \text{DELTA}) ** 2) \quad (37)$$

Summary of wave-equation formulas

Assume that we know the velocity, force function, and any other desired variable, for each segment at the "present" time (from previous computation or initial conditions). The same information for each segment is sought at a "future" time, DELTA in advance of the "present" time. To aid in the statement of variable names consider the suffix 2 as representing a condition at that "future" time, and 1 a condition at the "present".

As will be seen shortly, knowledge of the velocity V2 and the force function FCTN2 for each segment constitutes a complete solution to the problem. At the point of intersection of two characteristics

$$V2(I) + \text{FCTN2}(I) = V1(I-1) + \text{FCTN1}(I-1) \quad (38)$$

and

$$V2(I) - \text{FCTN2}(I) = V1(I+1) - \text{FCTN1}(I+1) \quad (39)$$

With the unknowns expressed explicitly

$$V2(I) = 0.5*(V1(I-1) + V1(I+1) + \text{FCTN1}(I-1) - \text{FCTN1}(I+1)) \quad (40)$$

and

$$\text{FCTN2}(I) = 0.5*(V1(I-1) - V1(I+1) + \text{FCTN1}(I-1) + \text{FCTN1}(I+1)) \quad (41)$$

for an interior segment.

The expression for an end segment comes by choosing a meaningful

characteristic equation and introducing the accompanying boundary condition. For example at the fixed end

$$V_2(M) = 0 \tag{42}$$

and

$$FCTN_2(M) = V_1(M-1) + FCTN_1(M-1) \tag{43}$$

It should not be assumed, however, that because of the discrete-segment nature of the model that it gives rise to a finite-difference approximation. The solution describing elastic behavior is an exact one.

Once obtained, FCTN permits the calculation of many other variables. The force, F , comes directly from the definition

$$df = \frac{dF}{c} = \frac{dF}{\sqrt{km}} \tag{44}$$

Arbitrarily let $f = 0$ when $F = F_0$ (the initial force of precompression) so that

$$f = \frac{F - F_0}{\sqrt{km}} \tag{45}$$

Solve for the force F , which for the I th segment is

$$F(I) = F_0 + KMROOT * "FCTN"(I) \tag{46}$$

where $KMROOT$ is a variable name representing the parameter \sqrt{km} . To obtain the force at the end of the time step, use $FCTN_2(I)$. For the average force during the time step, use $0.5*(FCTN_2(I) + FCTN_1(I))$.

A recursion formula for displacement can be developed from a formula expressing the length of a single segment.



Figure 14

The elastic force at the center of the Ith segment is related to its change in length by the finite difference approximation

$$(M-1)k[\Delta L_0 - \Delta L] = F - F_0 = \sqrt{km} f \quad (47)$$

from which

$$\Delta L = \Delta L_0 - \frac{\sqrt{m/k}}{M-1} f \quad (48)$$

Note that the coefficient of f is our choice for Δt .

$$\Delta L = \Delta L_0 - \Delta t f \quad (40)$$

The displacement of the Ith segment can therefore be obtained from the displacement of its neighbor.

$$X2(I) = XI-1) + DELLO - DELT*(FCTN2(I-1) + FCTN2(I))*0.5 \quad (50)$$

It should be clear that the variable FCTN is in itself a suitable measure of local density. If computation with wave-equation formulas continually produces values of FCTN2 less than some limiting value, say FCTMAX, rigid-body formation is absent and coil closure does not occur. However, any values of FCTN2 computed by the wave equation which exceed the limiting value imply the need for correction with rigid-body-motion equations.

Another property of FCTN is that its correct value within a rigid region always equals FCTMAX even if large internal forces occur during collisions. Once a rigid body forms, disturbances are propagated instantaneously throughout its length; the celerity becomes infinite, in which case

$$FCTN = \int_{F_0}^F \frac{dF}{\sigma c} = FCTMAX + \frac{1}{\sigma_{max}} \int_{F_{max}}^F \frac{dF}{c} \text{ rigid body} = FCTMAX \quad (51)$$

max (elastic)

Computational scheme

Although the rigid-body-motion equations have yet to be discussed, the basis of the computational scheme can still be presented. Whether or not rigid regions are already present or apt to form during the time step, each segment of the spring is treated as though wave-equation behavior were expected. Each segment is temporarily given the capacity to deform without limit.

an internal elastic force, embodied in FCTN, takes on whatever value is necessary to satisfy the characteristic equations. This is accomplished in the subroutine called SPRING.

If a rigid region were forming during this time step, one or more values of FCTN2 would equal or exceed its limiting value. Regions where this occurs are then detected and their component segments allowed to expand to the limiting size. Such rigid regions may be attached to either the moving or fixed end or may be floating freely in between -- each case requiring different treatment. This function of "detection" and further "direction" is performed by the subroutine CONTRL.

Before turning to the discussion of rigid-body motion it is important to realize what happens to existing rigid regions when operated upon by the wave equations. Wave-equation behavior is exhibited wherever the internal forces are entirely elastic. Significant forces arising out of inter-coil contact occur only when a rigid region is forming or growing in size. For a segment already confined within a rigid region, say the Ith segment, the characteristic equations report $FCTN2(I) = FCTMAX$ since $V1(I-1) = V1(I+1)$ and $FCTN1(I-1) = FCTN1(I+1) = FCTMAX$. Retaining its rigid property, the subroutine CONTRL will cause this region to be re-examined by the appropriate rigid-body-motion formulas.

Of course, a segment on one (or both) end(s) of an already existing rigid region may be shed upon application of the characteristic equations. In fact this is the manner in which a rigid region diminishes in size. Clearly, inasmuch as parameters were selected so that a disturbance propagates but one segment per time step, no more than one segment will be shed from a rigid region during that time step.

Rigid-body motion

For the sake of stability, two parameters identify the condition of rigid-body motion. Whenever a segment becomes rigid its force function is assigned a value FCTMAX. Subsequent testing for continuance of the rigid condition is done by comparing FCTN2 with FCTLIM, which is slightly less than FCTMAX. FCTLIM differs from FCTMAX only in the last significant figure, and

simply prevents round-off error from allowing a rigid segment to go undetected.

The subroutine CONTRL now directs the calling of three final subroutines, MOVRIg, FIXRIg, and MIDRIg, all of which employ finite-difference approximations to the rigid-body-motion equations. Though the wave equations placed no lower limit on the number of segments desired, it now appears that DELT should be chosen small enough to provide a sufficient number of segments to satisfy the demands of the following finite-difference approximations.

In the following sections the three cases of rigid-body motion are discussed in detail.

Rigid region attached to moving end; CALL MOVRIg

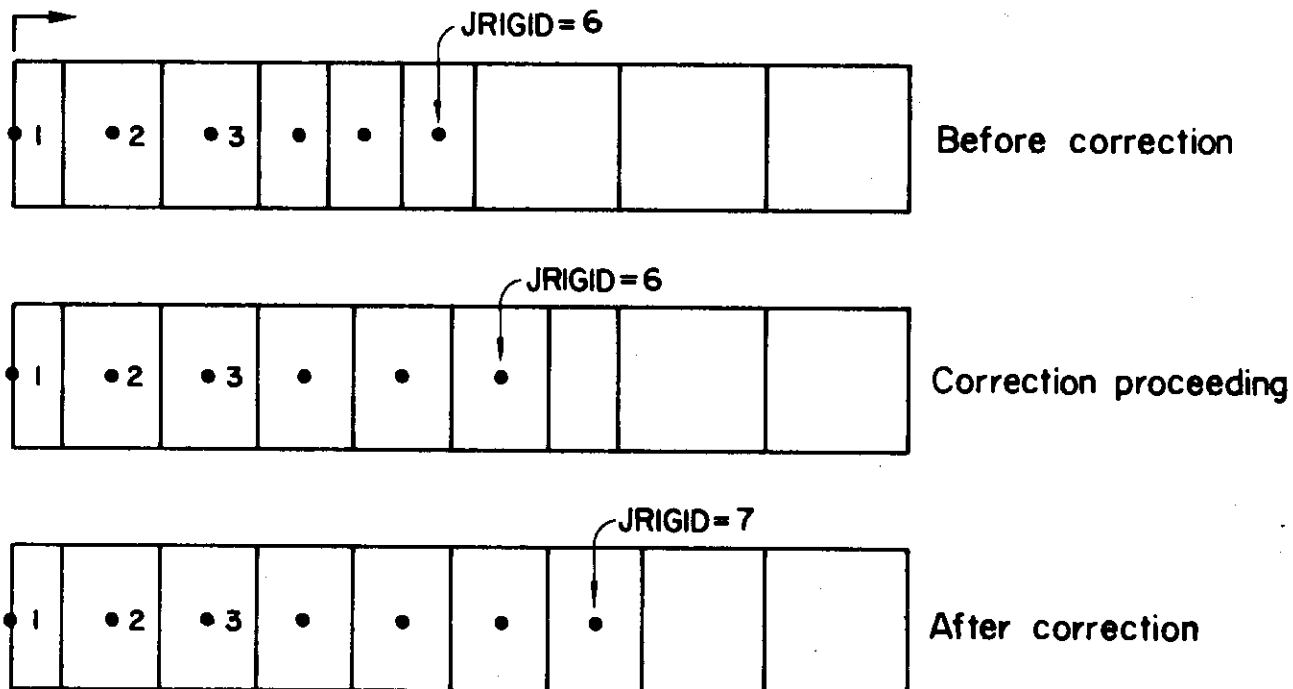


Figure 15

Consider the case where a rigid region has been detected at the moving end. Suppose, as illustrated in the above figure, that application of the wave equation has caused three more segments (4, 5, & 6) to become attached to the moving rigid region originally consisting of 2 1/2 segments

(1, 2, & 3). Let the thickness of each segment indicate the qualitative value for FCTN2.

$$\begin{aligned}
 &FCTN2(1) = FCTN2(2) = FCTN2(3) = FCTMAX \\
 &\left. \begin{array}{l} FCTN2(4) \\ FCTN2(5) \\ FCTN2(6) \end{array} \right\} > FCTLIM \quad FCTN2(7) < FCTLIM \quad (52)
 \end{aligned}$$

The variable JRIGID is used to identify the number of the anticipated terminal segment of the rigid region. In this example JRIGID = 6. The topmost portion of the above figure, labeled "Before correction", illustrates the condition of the spring as the subroutine MOVRIG assumes control over the computations.

Corrections begin by setting FCTN2 equal to FCTMAX for all segments which compose the rigid region delimited by JRIGID. Since reassigning the force function alters the thickness of a segment, the right-hand margin of the rigid region is evidently expanded further out into the field of elastic segments. The example in the middle portion of the above figure, labeled "Correction proceeding", illustrates this first step in the correction. Furthermore, as a consequence of this correction, segment no. 7 appears to be compressed beyond its allowable limit.

Corrections continue by checking whether or not JRIGID should be incremented by 1 -- whether or not another segment has been incorporated by the growing rigid region. The answer lies in examining the (revised) value of FCTN2(JRIGID+1).

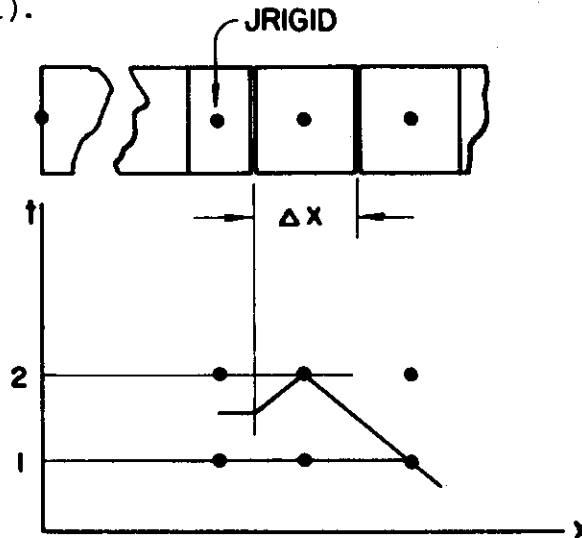


Figure 16

The proximity of the rigid body precludes the exclusive use of the characteristic equations in solving for segment JRIGID+1. Just how the characteristic line should approach from the left is open to some question. A simple calculation related to the thickness Δx is instead developed.

Δx is of course related to $FCTN2(JRIGID+1)$ as shown previously,

$$\Delta x = DELLO - DELT * FCTN2(JRIGID+1) \quad (53)$$

Δx is also dependent upon the "known" positions of neighboring segments. On the left: the position of the current candidate to be identified by JRIGID has already been corrected. On the right: unless the rigid region is shown to be even greater in extent, the disturbance will not propagate through more than one elastic segment during this time step. Segment JRIGID+2 has been solved by the wave equation.

$$\begin{aligned} \Delta x = \{ & X2(JRIGID+2) - 0.5 * (DELLO - DELT * FCTN2(JRIGID+2)) \} \\ & - \{ X2(1) + (FLOAT(JRIGID) - 0.5) * DELMIN \} \end{aligned} \quad (54)$$

Herein DELMIN is the minimum thickness of a segment. Equate expressions for Δx , and solve for $FCTN2(JRIGID+1)$

$$\begin{aligned} FCTN2(JRIGID+1) = & (1.5 * DELLO - (X2(JRIGID+2) - X2(1)) \\ & - (FLOAT(JRIGID) - 0.5) * DELMIN) / DELT - 0.5 * FCTN2(JRIGID+2) \end{aligned} \quad (55)$$

If $FCTN2(JRIGID+1) < FCTLIM$, the rigid region is isolated. If the contrary is true, include this segment by incrementing JRIGID by 1 segment, and check the new neighboring segment. The example concluded in the bottom-most portion of figure 15, labeled "After correction", illustrates that the inclusion of one more segment, no. 7, completes the correction.

All velocities, $V2$'s, in the moving rigid region are now assigned the boundary value $V2(1)$. The velocity of segment JRIGID+1 can be obtained from the one unquestioned characteristic equation

$$V2(JRIGID+1) = FCTN2(JRIGID+1) + V1(JRIGID+2) - FCTN2(JRIGID+2) \quad (56)$$

Displacements of all segments can be obtained from the same recursion formula developed previously for wave-equation behavior.

The average force centered within segment JRIGID+1 during the time

step, since the segment is wholly elastic, is obtained directly from the force functions

$$F(JRIGID+1) = FO + KMROOT*(FCTN2(JRIGID+1) + FCTN1(JRIGID+1))*0.5 \quad (57)$$

The corresponding forces in the rigid body are obtained by a finite-difference approximation to the momentum equation. This is accomplished by a recursion formula from segment no. JRIGID

$$F(I) = F(I+1) + DMDT*(V2(I+1) + V2(I) - V1(I+1) - V1(I))*0.5 \quad (58)$$

Rigid region attached to fixed end; CALL FIXRIG

The detection and correction of a rigid region that has formed at the fixed end proceeds in exactly the same manner as discussed above for the moving end. It will suffice to summarize the formulas used.

The variable IRIGID is used to identify the number of the anticipated terminal segment of the rigid region. To check whether or not IRIGID should be decremented by 1 -- whether or not yet another segment has been incorporated by the growing rigid region -- FCTN2(IRIGID-1) is revised and examined.

$$FCTN2(IRIGID-1) = (1.5*DELLO - (X2(M) - FLOAT(M-IRIGID) + 0.5)*DELMIN - X2(IRIGID-2))/DELT - 0.5*FCTN2(IRIGID-2) \quad (59)$$

With corrections completed, all velocities V2's in the fixed rigid region are assigned the boundary value 0 (zero). The velocity of segment IRIGID-1 can be obtained from

$$V2(IRIGID-1) = -FCTN2(IRIGID-1) + V1(IRIGID-2) - FCTN2(IRIGID-2) \quad (60)$$

The average forces within the rigid body during the time step are obtained by a recursion formula

$$F(I) = F(I-1) - DMDT*(V2(I-1) - V1(I) - V1(I-1))*0.5 \quad (61)$$

Rigid region floating freely; CALL MIDRIG

The same basic ideas used for correcting attached rigid regions

permeate the correction process for a free-floating rigid region. As before, the segments are allowed to expand and occupy their limiting size, and it is determined whether or not adjacent segments are incorporated into the rigid region. However, the computation is complicated by the absence of a simple reference fixing some position in the rigid region.

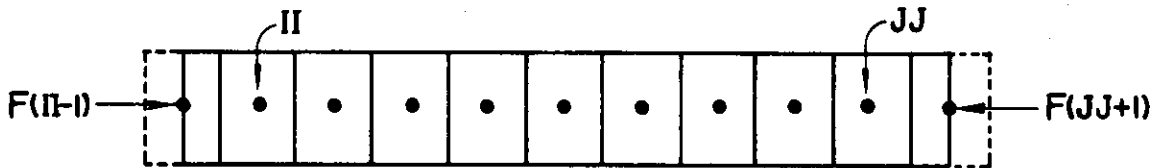


Figure 17

Consider the accompanying free-body and proceed to apply the impulse-momentum equation for the period covered by the time step. Two variables, II and JJ, are used to identify the numbers of the anticipated respectively left and right terminal segments of the rigid region. The sum of the initial velocities of all segments so included in the rigid body is given the variable name VLSUM

$$VLSUM = \sum_{I=II}^{JJ} V1(I) \quad (62)$$

Next, solve for

$$VRIG2 = V2(II) = V2(II+1) = \dots = V2(JJ) \quad (63)$$

The sum of the external impulses is equated to the change in momentum.

$$[F(II-1) - F(JJ+1)]\Delta t = \Delta m[(JJ-II+1)*VRIG2 + 0.5*(V2(II-1) + V2(JJ+1))] - \Delta m[VLSUM + 0.5*(V1(II-1) + V1(JJ+1))] \quad (64)$$

Herein Δm is the (constant) mass of any one segment. Of course, with segments II-1 and JJ+1 presumed to be elastic, the force function can be introduced

$$[F(II-1) - F(JJ+1)]\Delta t = [(FCTN2(II-1) + FCTN1(II-1) - FCTN2(JJ+1) - FCTN1(JJ+1))*0.5 \sqrt{km}]\Delta t \quad (65)$$

Equate the right-hand sides of both equations, and in doing so recognize that

$$\Delta t = \frac{\sqrt{m/k}}{M-1} \quad \text{or} \quad \sqrt{km} \Delta t = \frac{m}{M-1} = \Delta m \quad (66)$$

which permits cancellation of some parameters. Solve for VRIG2 to yield

$$\begin{aligned} \text{VRIG2} = & (0.5*(\text{FCTN2}(\text{II}-1) + \text{FCTN1}(\text{II}-1) - \text{FCTN2}(\text{JJ}+1) - \text{FCTN1}(\text{JJ}+1) \\ & - \text{V2}(\text{II}-1) + \text{V1}(\text{II}-1) - \text{V2}(\text{JJ}+1) + \text{V1}(\text{JJ}+1)) + \text{VLSUM})/\text{FLOAT}(\text{JJ}-\text{II}+1) \end{aligned} \quad (67)$$

VRIG2 can now be used to fix a position, viz. the center of mass, of the rigid region. The sum of the initial positions of these segments is given the variable name XLSUM

$$\text{XLSUM} = \sum_{\text{I}=\text{II}}^{\text{JJ}} \text{X1}(\text{I}) \quad (68)$$

The position of the center of mass at the end of the time step becomes

$$\text{XRIG2} = \text{XLSUM}/\text{FLOAT}(\text{JJ}-\text{II}+1) + 0.5*(\text{VRIG2} + \text{VLSUM}/\text{FLOAT}(\text{JJ}-\text{II}+1))*\text{DELT} \quad (69)$$

Now the estimated position of each end of the rigid region can be specified.

$$\text{X2}(\text{II}) = \text{XRIG2} - \text{DELMIN}*\text{FLOAT}(\text{JJ}-\text{II})/2. \quad (70)$$

$$\text{X2}(\text{JJ}) = \text{XRIG2} + \text{DELMIN}*\text{FLOAT}(\text{JJ}-\text{II})/2. \quad (71)$$

These final expressions reflect the first step in rigid body correction, expansion of segments to occupy their limiting size.

What now of the segments adjacent to this rigid region? Treatment of the right-hand end of a floating rigid region is no different than the (right-hand) end of the rigid region attached to the moving end. Few changes are needed as the formula for segment JRIGID+1 is employed for JJ+1.

$$\begin{aligned} \text{FCTN2}(\text{JJ}+1) = & (1.5*\text{DELLO} - (\text{X2}(\text{JJ}+2) - \text{XRIG2} - (\text{FLOAT}(\text{JJ}-\text{II})/2. \\ & + 0.5)*\text{DELMIN}))/\text{DELT} - 0.5*\text{FCTN2}(\text{JJ}+1) \end{aligned} \quad (72)$$

Similarly, the formula for segment IRIGID-1 undergoes little change in this new role

$$\begin{aligned} \text{FCTN2}(\text{II}-1) = & (1.5*\text{DELLO} - (\text{XRIG2} - (\text{FLOAT}(\text{JJ}-\text{II})/2. + 0.5) \\ & *\text{DELMIN} - \text{X2}(\text{II}-2)))/\text{DELT} - 0.5*\text{FCTN2}(\text{II}-2) \end{aligned} \quad (73)$$

Explicit expressions for the unknowns are lacking in this collection of formulas. Consequently, they are obtained by an iterative solution. In the order stated, the formulas for VRIG2, XRIG2, and FCTN2's for the adjacent segments are cycled until the iterations produce unvarying values.

If only one of the two adjacent segments exhibits a force function in excess of the limiting value, the corresponding segment is included in the rigid region, and the entire correction process is repeated. If both adjacent segments appear to require correction, only the segment showing the more severe error (i.e. the larger value of FCTN2) is corrected at that stage. This procedure appears wise in that upon adjustment of one end of the rigid region, the estimate of FCTN2 at the other is altered. Perhaps a marginal value of FCTN2 would cause a segment to be erroneously included in the rigid region should a less careful criterion be applied, and once included, no mechanism exists to shed the segment until the next time step.

Floating rigid regions are apt to arise in the proximity of, or even become attached to, the ends of the spring. The checking of the half-segments thus encountered demands special formulas. Their development, which is fundamentally the same as others discussed previously, requires recognition of the special geometry encountered.

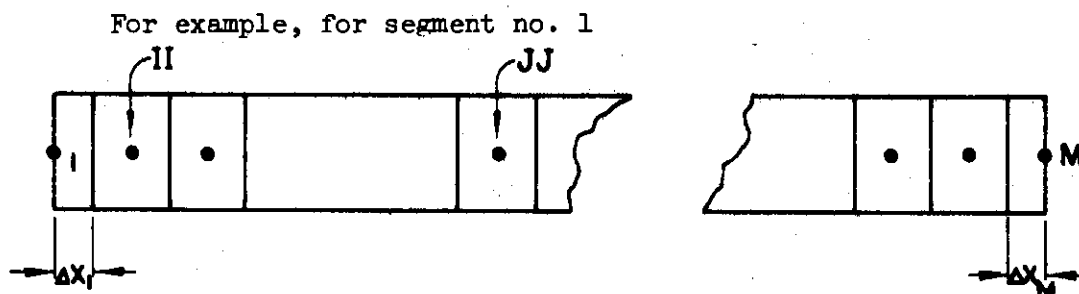


Figure 18

The half-segment thickness can be expressed in two ways:

$$\Delta x_1 = 0.5 * [DELLO - DELT * FCTN2(1)] \quad (74)$$

or

$$\Delta x_1 = \{XRIG2 - DELMIN * (FLOAT(JJ-II)2. + 0.5)\} - \{X2(1)\} \quad (75)$$

Upon eliminating Δx_1

$$FCTN2(1) = (DELLO - 2 * (XRIG2 - DELMIN * (FLOAT(JJ-II)/2. + 0.5) - X2(1))) / DELT \quad (76)$$

Similarly, for segment no. M

$$FCTN2(M) = (DELLO - 2.*(X2(M) - XRIG2 - DELMIN*(FLOAT(JJ-II)/2. + 0.5)))/DELT \quad (77)$$

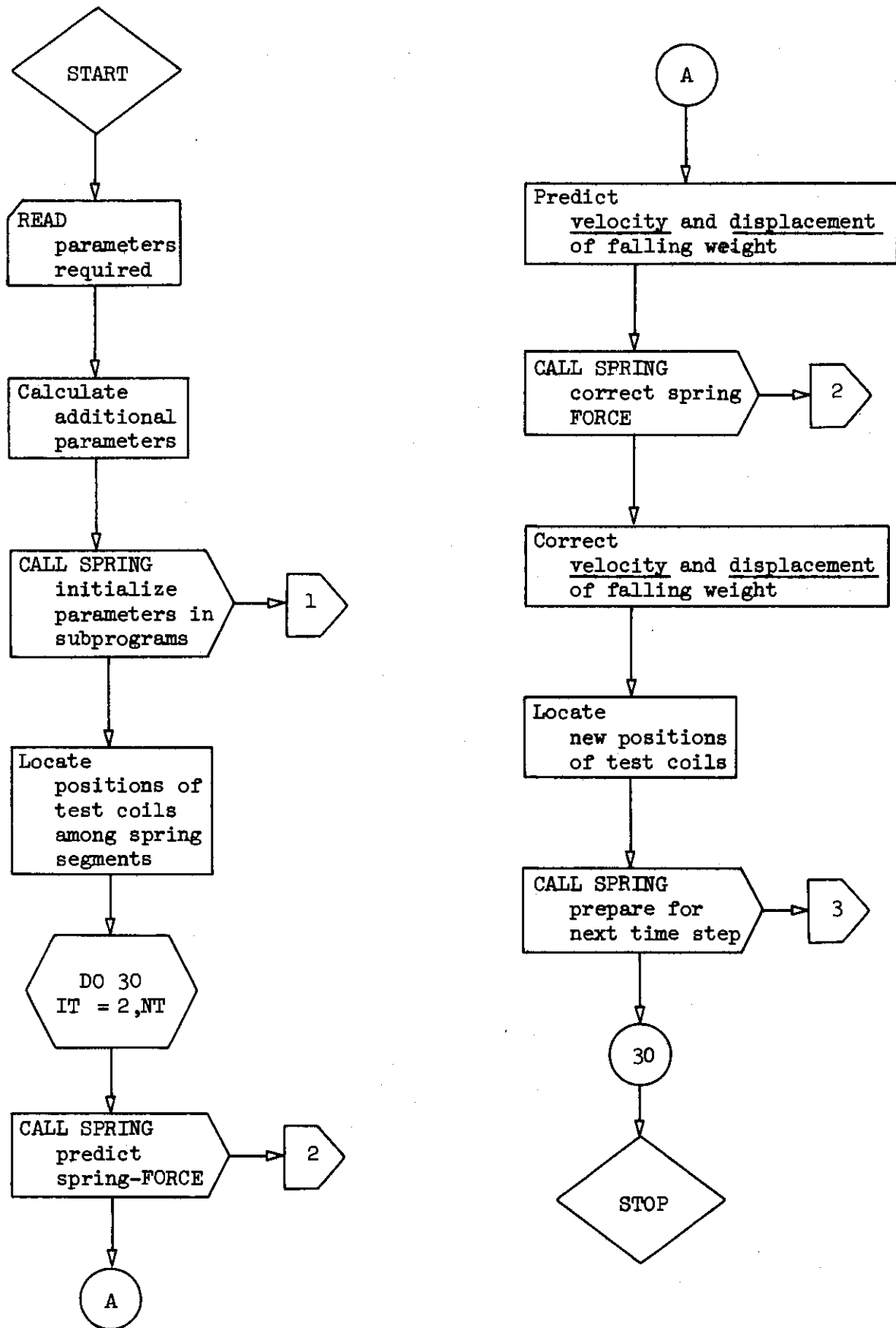
Fully compressed spring

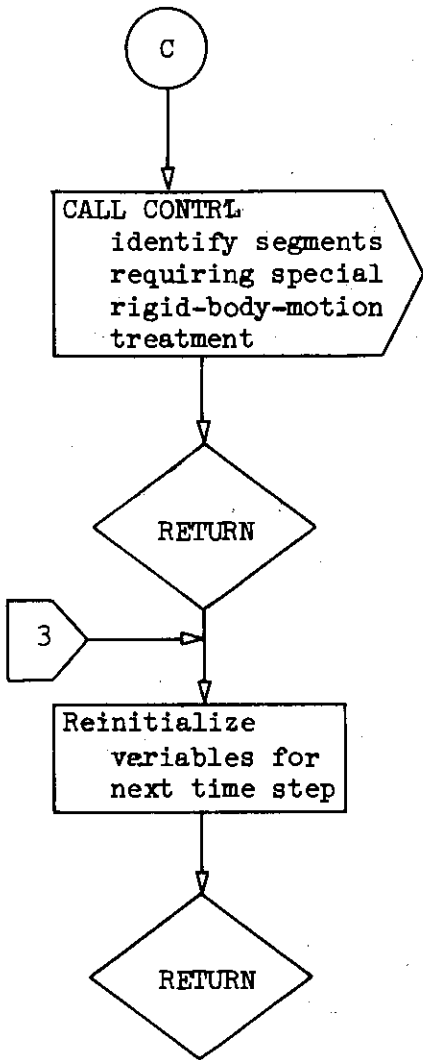
The resulting program can follow the formation of rigid regions up to the point where the spring becomes completely compressed. At this point computation ceases. If, however, one wishes to continue study of this case and examine the expansion phase, it is only necessary to reload the program, specifying as initial conditions, a spring at maximum precompression.

Flow charts

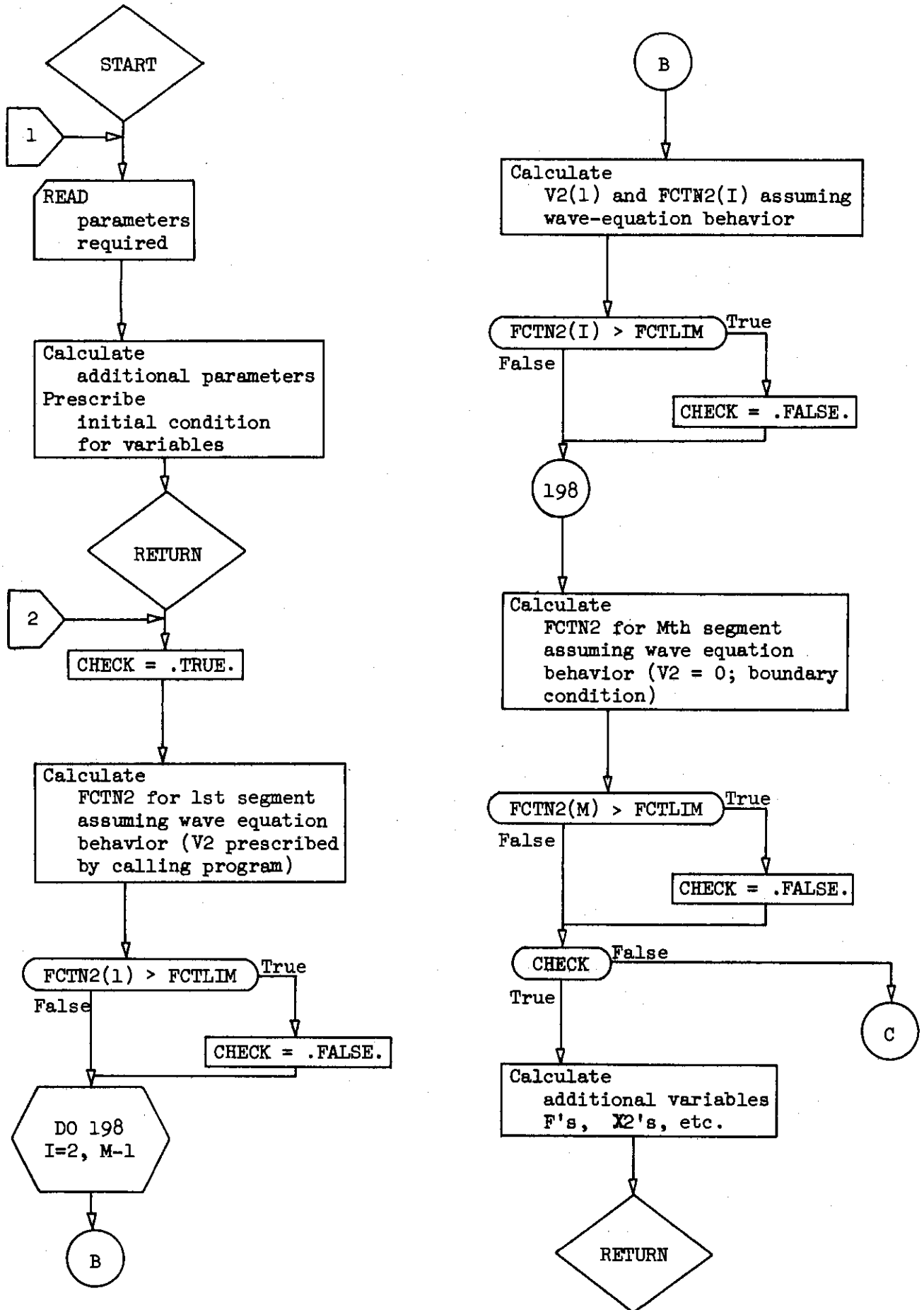
The accompanying set of flow charts offers the reader more insight into the logic and ordering of the computation. Excessive detail has given way to general statements wherever such detail appeared to obscure the picture. Details are important nonetheless, and the interested reader can glean them from the complete FORTRAN listings which appear in the appendix.

Main Program -- Spring Experiment

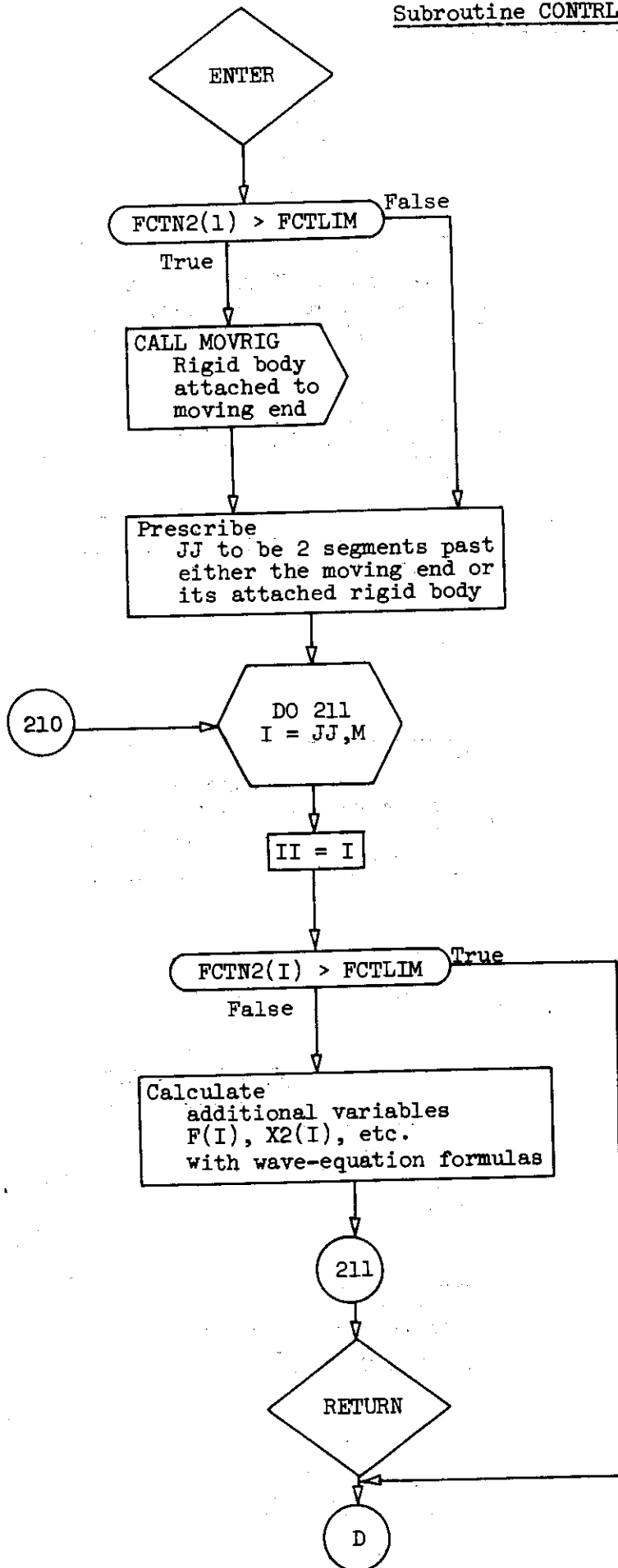




Subroutine SPRING



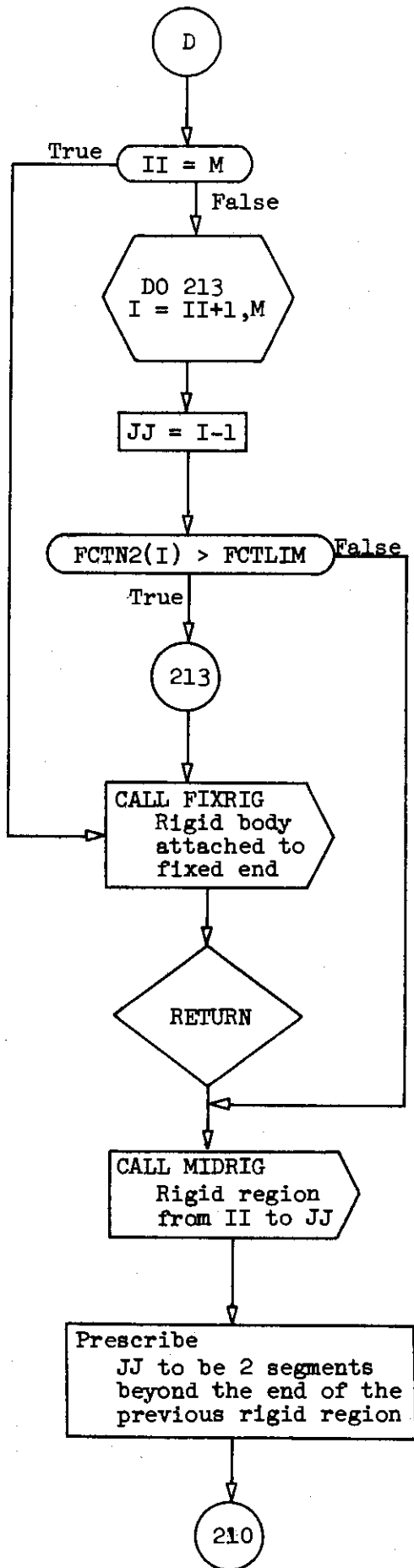
Subroutine CONTRL



Search initiated for floating rigid region.

Locate the beginning of the rigid region. Identify it with II.

Loop completed? No rigid region detected in last search.



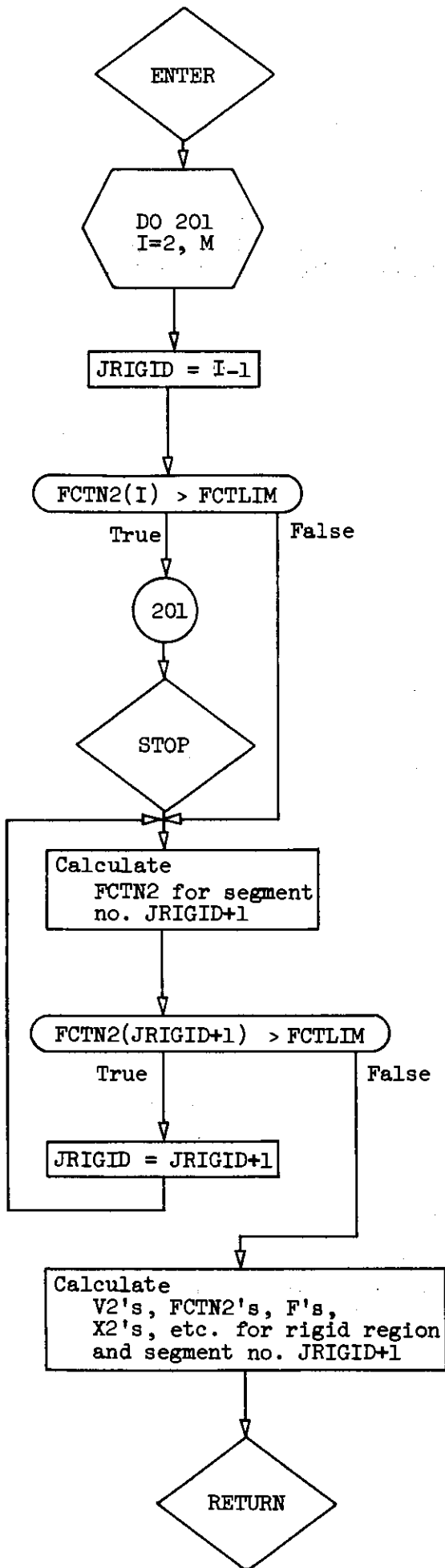
Locate the end of the rigid region. Identify it with JJ.

Rigid region is attached to fixed end.

Rigid region isolated from II to JJ (inclusive).

Search resumed for another floating rigid region.

Subroutine MOVRI

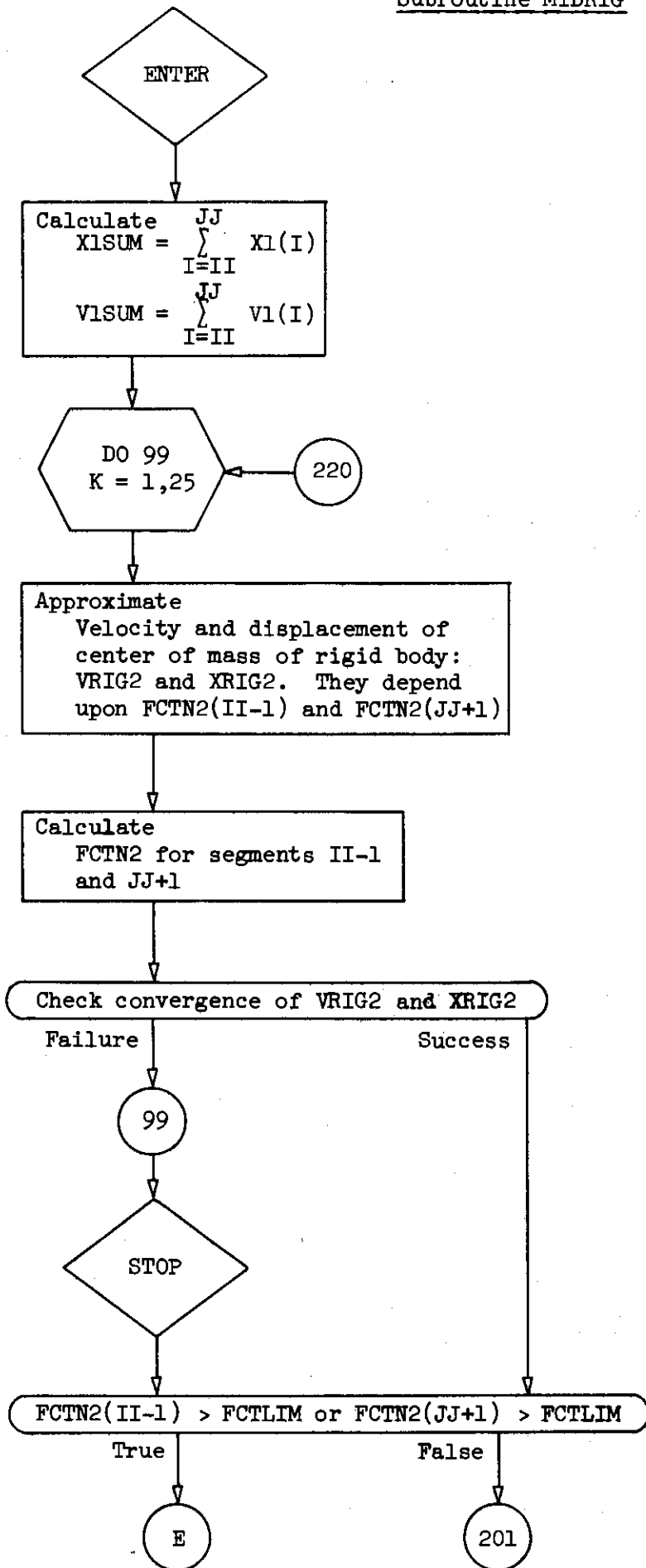


Approximate end of rigid region attached to moving end. Identify it with JRIGID.

Loop completed? Spring compressed solid.

Check whether additional adjacent segments become rigid and attached to moving end. Special treatment given if Mth segment must be checked.

Subroutine MIDRIG



Rigid region isolated from II to JJ (inclusive) given by calling program

Parameters necessary to apply rigid-body-motion equations

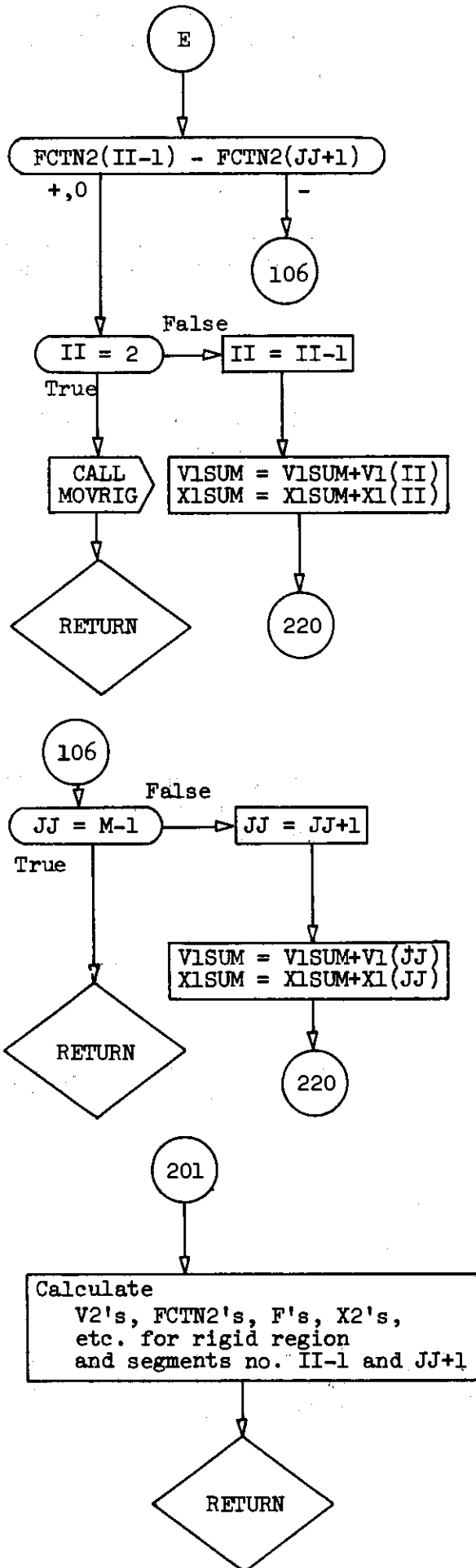
Limit following iterations to (say) 25

Special treatment given if 1st or Mth segments must be calculated

Loop completed? Failure to converge on values for VRIG2 and XRIG2

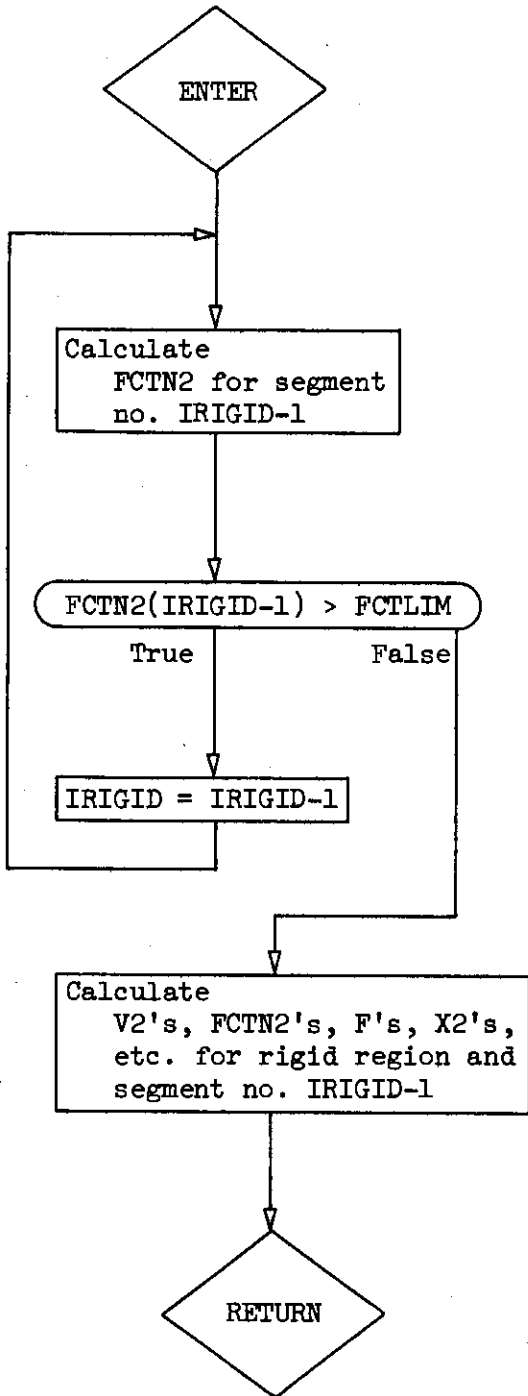
Check whether an adjacent segment becomes attached to rigid body

Add segment to end showing
the most severe error



RETURN to CONTRL and CALL
FIXRIG from there

Subroutine FIXRIG



Approximate end of rigid region attached to fixed end supplied by calling program. Identify it with IRIGID.

Check whether additional adjacent segments become rigid and attached to fixed end. Special treatment given if 1st segment must be checked.

```

C   SPRING EXPERIMENT
    REAL MTOT
    COMMON DELT,DELT2,INTV,M,DEL,XSEG(100)
    DIMENSION SEG(4), ISEG(4), PART(4)
    READ(5,100) W1,W2,DROP,DELT,NT,INTV
100  FORMAT(4F10.5,2I5)
    READ(5,99) NSEG, (SEG(J),J=1,NSEG)
    99  FORMAT(I5,4F10.5)
C   CALCULATE PARAMETERS
    DELT2 = 0.5*DELT
    WTOT = W1 + W2
    MTOT = WTOT/(12.*32.2)
    V1 = SQRT(64.4*12.*DROP)*W1/WTOT
    X1 = 0.
    CALL SPRING(1,FORCE,V1,X1)
    J = 1
    DO 300 I=1,M
    IF(XSEG(I).LE.SEG(J)) GO TO 300
    ISEG(J) = I - 1
    PART(J) = (SEG(J) - XSEG(I-1))/DEL
    IF(J.EQ.NSEG) GO TO 301
    J = J + 1
300  CONTINUE
301  WRITE(6,200) W1,DROP,W2,V1
200  FORMAT(/56H      OTHER CHARACTERISTICS OF THE SYSTEM -- WEIGHT W1 =
1 F7.3,27H FALLING FROM A HEIGHT OF F7.3,20H ON TO WEIGHT W2 =
2 F7.3/44X,33HPRODUCING AN INITIAL VELOCITY OF F10.5/)
CARD CAN BE REVERSED TO SUPPRESS WRITE STATEMENT
    WRITE(6,199) (ISEG(J), PART(J), J=1,NSEG)
199  FORMAT(53X,4(I2,2H +,F7.4,4X))
    V2 = V1
    X2 = 0.
    TIM = 0.
CARD CAN BE REVERSED TO SUPPRESS WRITE STATEMENT
    WRITE(6,202) TIM, V2, X2, (SEG(J),J=1,NSEG)
    DO 30 IT=2,NT
    TIM = FLOAT(IT - 1)*DELT
    V = V1 + (WTOT - FORCE)*DELT/MTOT
    DO 20 L=1,2
    X = X1 + (V1 + V)*DELT2
    CALL SPRING(2,FORCE,V,X)
    V2 = V1 + (WTOT - FORCE)*DELT/MTOT
20  V = V2
21  X2 = X1 + (V1 + V2)*DELT2
    V1 = V2
    X1 = X2
    DO 310 J=1,NSEG
    I = ISEG(J)
310  SEG(J) = XSEG(I) + PART(J)*(XSEG(I+1) - XSEG(I))

```

```

CALL SPRING(3, FORCE, V1, X1)
CARD CAN BE REVERSED TO SUPPRESS WRITE STATEMENT
  IF((IT-1)/INTV*INTV.EQ.IT-1) WRITE(6,203) IT, TIM, V2, X2, (SEG(J),
  1 J=1, NSEG)
30 CONTINUE
202 FORMAT(12X, 4HTIME, 9X, 8HVELOCITY, 5X, 12HDISPLACEMENT//4H 1, 5X,
  1 F10.5, 6(5X, 1PE10.3))
203 FORMAT(/1X, I3, 5X, F10.5, 6(5X, 1PE10.3))
CALL EXIT
END

```

```

SUBROUTINE SPRING(NICHE, FORCE, V, X)
COMMON DELT, DELT2, LINT, M, DELLO, X2(100)
LOGICAL RIGID, CHECK
REAL MASS, K, KMASS, KMROOT, LO, LENGTH, LMIN, MV, MV1, KTRY
COMMON /ONE/ RIGID(100), F(100), FCTN1(100), FCTN2(100), V1(100),
  1 V2(100), X1(100), SIG(100), FCTLIM, FCTMAX, SIGMAX, DELMIN, DMDT, DELM,
  2 KMRCOT, FO, JRIGID, IRIGID
GO TO(901, 902, 903), NICHE
901 READ(5, 1000) MASS, LENGTH, K, LO, LMIN, NSTEP
1000 FORMAT(5F10.5, I5)
M = SQRT(MASS/K)/DELT + 1.5
MM1 = M - 1
KTRY = K
K = MASS/((FLOAT(MM1)*DELT)**2)
FO = K*(LENGTH-LO)
KMASS = K*MASS
KMROOT = SQRT(KMASS)
DELM = MASS/FLOAT(MM1)
DELLO = LO/FLOAT(MM1)
DMDT = DELM/DELT
DELMIN = LMIN/FLOAT(MM1)
SIGMAX = DELM/DELMIN
FMAX = K*(LENGTH - LMIN)
FCTMAX = (FMAX - FO)/KMROOT
FCTLIM = FCTMAX*0.999999
WGT = MASS*12.0*32.2
WRITE(6, 1001) WGT, LENGTH, LMIN, LO, K, KTRY, FMAX, DELT, LINT, M
1001 FORMAT(49H1 BASIC UNITS ARE POUNDS, INCHES, AND SECONDS./
  143H0 SPRING CHARACTERISTICS -- TOTAL WGT. =F10.3, 23H UNSTRETCH
  2ED LENGTH = F10.5/30X, 17H MINIMUM LENGTH =F9.5, 21H INITIAL LENG
  3TH = F10.5/30X, 18H SPRING CONSTANT =F10.5, 3H (, F10.5, 9H READ IN),
  4 22H MAX. ELASTIC FORCE = F9.2/20H TIME INTERVAL = F10.5,
  5 21H WITH RESULTS EVERY 15, 10H INTERVALS/29H NUMBER OF MESH P
  60INTS = , I5)
C INITIAL CONDITION OF THE SPRING

```

```

DO 111 I=1,M
RIGID(I) = .FALSE.
F(I) = F0
FCTN1(I) = 0.0
V1(I) = 0.
SIG(I) = DELM/ DELLO
X1(I) = FLOAT(I-1)*DELLO
111 X2(I) = X1(I)
V1(1) = V
V2(M) = 0.
SUM = 0.
MVI = 0.5*DELM*V
TIME = 0.0
WRITE(6,1003) TIME,(I,V1(I),X1(I),FCTN1(I),SIG(I),F(I),I=NSTEP,
1 MM1,NSTEP),M,V1(M),X1(M),FCTN1(M),SIG(M),F(M)
1003 FORMAT (1H 10H      TIME=F9.6/(24X,I5,E15.8,F10.4,E15.8,F14.7,
1 F7.0))
KOUNT = 0
FORCE = F(1)
RETURN
C COMPUTE SPRING MOTION
902 CHECK = .TRUE.
C CALCULATE FOR I = 1
I = 1
V2(1) = V
X2(1) = X
FCTN2(1) = FCTN1(2) - V1(2) + V2(1)
JRIGID = 0
IRIGID = M + 1
IF(FCTN2(1) .LE. FCTLIM) GO TO 199
CHECK = .FALSE.
FCTN2(1) = FCTMAX
C CALCULATE FOR I .GT. 1
199 I = I+1
IF(I.EQ.M) GO TO 198
C WAVE EQUATION BEHAVIOR
V2(I) = 0.5*(V1(I-1)+V1(I+1)+FCTN1(I-1)-FCTN1(I+1))
FCTN2(I) = 0.5*(V1(I-1)-V1(I+1)+FCTN1(I-1)+FCTN1(I+1))
IF(FCTN2(I) .LE. FCTLIM) GO TO 199
FCTN2(I) = FCTMAX
CHECK = .FALSE.
GO TO 199
198 V2(M) = 0.0
RIGID(M) = .FALSE.
FCTN2(M) = FCTN1(M - 1) + V1(M - 1)
IF(FCTN2(M) .LE. FCTLIM) GO TO 197
FCTN2(M) = FCTMAX
CHECK = .FALSE.
197 IF(CHECK) GO TO 298

```

MOMENTUM
MOMENTUM

WRITEOUT

CALL CONTRL
RETURN

```

C ALL SEGMENTS ARE FLEXIBLE
298 RIGID(1) = .FALSE.
   SIG(1) = DELM/(DELLO - DELT*FCTN2(1))
   F(1) = F0 + KMROOT*(FCTN2(1) + FCTN1(1))*0.5
   DO 299 I = 2,M
   SIG(I) = DELM/(DELLO - DELT*FCTN2(I))
   DELL = DELLO - DELT*(FCTN2(I-1) + FCTN2(I))*0.5
   X2(I) = X2(I-1) + DELL
   RIGID(I) = .FALSE.
299 F(I) = F0 + KMROOT*(FCTN2(I) + FCTN1(I))*0.5
305 FORCE = F(1)
   RETURN

```

C RESET THE RESULTS OF THE SPRING

```

903 V1(1) = V2(1)
   X1(1) = X2(1)
   FCTN1(1) = FCTN2(1)
   MV = V1(1)*0.5
   DO 4 I=2,M
   X1(I) = X2(I)
   V1(I) = V2(I)
   MV = MV + V1(I)
4 FCTN1(I) = FCTN2(I)
   SUM = SUM + (F(1) - F(M))*DELT
   MV = DELM*MV - MV1
   TIME = TIME + DELT

```

MOMENTUM

MOMENTUM

MOMENTUM

MOMENTUM

CARD CAN BE REVERSED TO SUPPRESS WRITE STATEMENT

```

WRITE(6,1004) TIME,V1(1),X2(1),F(1),JRIGID,IRIGID,F(M),SUM,MV
1004 FORMAT (//11H          TIME=F9.6,10H,    V(1)=E15.6
1,10H,    X(1)=F10.4,10H,    F(1)=F7.0/10H, JRIGID=I4,10H, IRIGID
2=I4,10H,    F(M)=F7.0,2X,14HTOTAL IMPULSE=E15.8,20H    TOTAL MOME
3NTUM=E15.8)
KOUNT = KOUNT + 1
IF(KOUNT/LINT*LINT.NE.KOUNT) GO TO 2

```

WRITEOUT

WRITEOUT

CARD CAN BE REVERSED TO SUPPRESS WRITE STATEMENT

```

WRITE(6,1005) (I,V1(I),X2(I),FCTN1(I),SIG(I),F(I),RIGID(I),
1 I=NSTEP,MM1,NSTEP),M,V1(M),X2(M),FCTN1(M),SIG(M),F(M),RIGID(M)
1005 FORMAT(1H /24X,5H    I,10H    V(I),5X,10H    X(I) ,5X,10HFCTN1(
1I) ,14H    SIG(I)    ,7H F(I) ,7H RIGID //(24X,I5,E15.8,F10.4,E1
25.8,F14.7,F7.0,L7))
2 RETURN
END

```

C
C

SUBROUTINE CONTRL
COMMON DELT,DELT2,LINT,M,DELLO,X2(100)

```
LOGICAL RIGID
REAL KMROOT
COMMON /ONE/ RIGID(100),F(100),FCTN1(100),FCTN2(100),V1(100),
1 V2(100),X1(100),SIG(100),FCTLIM,FCTMAX,SIGMAX,DELMIN,DMDT,DELM,
2 KMROOT,F0,JRIGID,IRIGID
IF(FCTN2(1).LT.FCTLIM) GO TO 208
CALL MOVRIG
GO TO 209
C THE MOVING END IS FLEXIBLE
208 RIGID(1) = .FALSE.
SIG(1) = DELM/(DELLO - DELT*FCTN2(1))
F(1) = F0 + KMROOT*(FCTN2(1) + FCTN1(1))*0.5
209 JJ = JRIGID + 2
210 DO 211 I=JJ,M
II = I
IF(FCTN2(I).GT.FCTLIM) GO TO 212
SIG(I) = DELM/(DELLO - DELT*FCTN2(I))
DELL = DELLO - DELT*(FCTN2(I) + FCTN2(I-1))*0.5
X2(I) = X2(I-1) + DELL
F(I) = F0 + KMROOT*(FCTN2(I) + FCTN1(I))*0.5
211 RIGID(I) = .FALSE.
RETURN
212 IF(II.GE.M-1) GO TO 219
IIP1 = II + 1
DO 213 I=IIP1,M
JJ = I - 1
IF(FCTN2(I).GT.FCTLIM) GO TO 213
CALL MIDRIG(II, JJ)
GO TO 210
213 CONTINUE
219 CALL FIXRIG(II)
RETURN
END
```

```
SUBROUTINE MOVRIG
COMMON DELT,DELT2,LINT,M,DELLO,X2(100)
LOGICAL RIGID
REAL KMROOT
COMMON /ONE/ RIGID(100),F(100),FCTN1(100),FCTN2(100),V1(100),
1 V2(100),X1(100),SIG(100),FCTLIM,FCTMAX,SIGMAX,DELMIN,DMDT,DELM,
2 KMROOT,F0,JRIGID,IRIGID
C THE MOVING END IS RIGID
DO 201 I=2,M
JRIGID = I - 1
IF(FCTN2(I).LE.FCTLIM) GO TO 202
201 CONTINUE
```

```
GO TO 206
C   RECALCULATE FUNCTION AT THE LAST SEGMENT OF THE RIGID PART
C   ATTACHED TO THE MOVING END
202 IF(JRIGID.GE.M-1) GO TO 205
   X2(JRIGID+2) = X1(JRIGID+2) + (V2(JRIGID+2) + V1(JRIGID+2))*DELT2
   FCTN2(JRIGID+1) = ((1.5*DELLO - (X2(JRIGID+2) - X2(1) - DELMIN*
1 (FLOAT(JRIGID) - 0.5)))/DELT - 0.5*FCTN2(JRIGID+2)
   IF(FCTN2(JRIGID + 1) .LE. FCTLIM) GO TO 204
   JRIGID = JRIGID + 1
   GO TO 202
205 FCTN2(M) = (DELLO - 2.*(X2(M) - X2(1) - DELMIN*(FLOAT(M-2) +
1 0.5)))/DELT
   IF(FCTN2(M).LE.FCTLIM) GO TO 207
206 WRITE(6,200)
200 FORMAT(//24H SPRING COMPRESSED SOLID)
   CALL EXIT
204 V2(JRIGID+1) = V1(JRIGID+2) - FCTN1(JRIGID+2) + FCTN2(JRIGID+1)
   DELL = DELLO - DELT*(FCTMAX + FCTN2(JRIGID+1))*0.5
   X2(JRIGID+1) = X2(JRIGID) + DELL
207 RIGID(JRIGID+1) = .FALSE.
   SIG(JRIGID+1) = DELM/(DELLO - DELT*FCTN2(JRIGID+1))
   F(JRIGID+1) = FO + KMROOT*(FCTN2(JRIGID+1) + FCTN1(JRIGID+1))*0.5
C   COMPUTE MASS DENSITY,DISPLACEMENT,VELOCITY AND SPRING FORCE
C   FOR ALL RIGID SEGMENTS ATTACHED TO THE MOVING END
DO 203 II=1,JRIGID
  I = JRIGID + 1 - II
  V2(I) = V2(1)
  FCTN2(I) = FCTMAX
  RIGID(I) = .TRUE.
  SIG(I) = SIGMAX
  X2(I) = X2(1) + FLOAT(I - 1 )*DELMIN
203 F(I) = F(I+1) + DMDT*(V2(I+1) + V2(I) - V1(I+1) - V1(I))*0.5
RETURN
END
```

```
SUBROUTINE MIDRIG(II,JJ)
COMMON DELT,DELT2,LINT,M,DELLO,X2(100)
LOGICAL RIGID
REAL KMROOT, ERR/1.0E-05/
COMMON /ONE/ RIGID(100),F(100),FCTN1(100),FCTN2(100),V1(100),
1 V2(100),X1(100),SIG(100),FCTLIM,FCTMAX,SIGMAX,DELMIN,DMDT,DELM,
2 KMRCOT,FO,JRIGID,IRIGID
X1SUM = 0.0
V1SUM = 0.0
DO 221 I=II,JJ
X1SUM = X1SUM + X1(I)
```

```
221 VISUM = VISUM + V1(I)
    XTRY = 0.0
    VTRY = 0.0
220 DO 99 K=1,25
    VRIG2 = (0.5*(FCTN2(II-1) + FCTN1(II-1) - FCTN2(JJ+1) - FCTN1(JJ
1 +1) - V2(II-1) + V1(II-1) - V2(JJ+1) + V1(JJ+1)) + VISUM)/
2 FLOAT(JJ - II + 1)
    XRIG2 = X1SUM/FLOAT(JJ - II + 1) + (VRIG2 + VISUM/FLOAT(JJ - II
1 + 1))*DELT2
    IF(II.EQ.2) GO TO 100
    FCTN2(II-1) = (1.5*DELLO - (XRIG2 - DELMIN*(FLOAT(JJ - II)/2.
1 + 0.5) - X2(II-2)))/DELT - 0.5*FCTN2(II-2)
    V2(II-1) = FCTN1(II-2) + V1(II-2) - FCTN2(II-1)
    GO TO 101
100 FCTN2(1) = (DELLO - 2.*(XRIG2 - DELMIN*(FLOAT(JJ - II)/2. + 0.5)
1 - X2(1)))/DELT
101 IF(JJ.EQ.M-1) GO TO 102
    X2(JJ+2) = X1(JJ+2) + (V2(JJ+2) + V1(JJ+2))*DELT2
    FCTN2(JJ+1) = (1.5*DELLO - (X2(JJ+2) - XRIG2 - DELMIN*(FLOAT(JJ
1 - II)/2. + 0.5)))/DELT - 0.5*FCTN2(JJ+2)
    V2(JJ+1) = V1(JJ+2) - FCTN1(JJ+2) + FCTN2(JJ+1)
    GO TO 103
102 FCTN2(M) = (DELLO - 2.*(X2(M) - XRIG2 - DELMIN*(FLOAT(JJ -
1 II)/2. + 0.5)))/DELT
103 IF((ABS((XRIG2 - XTRY)/XRIG2).LE.ERR).AND.(ABS((VRIG2 - VTRY)/
1 VRIG2).LE.ERR)) GO TO 104
    IF(K - 20) 97,95,96
95 WRITE(6,94)
94 FORMAT(/4X,7HII    JJ,8X,4HVTRY,12X,5HVRIG2,13X,4HXTRY,12X,
1 5HXRIG2,10X,11HFCTN2(II-1),6X,11HFCTN2(JJ+1))
96 WRITE(6,1) II,JJ,VTRY,VRIG2,XTRY,XRIG2,FCTN2(II-1),FCTN2(JJ+1)
1  FORMAT(1X,2I5,6(3X,1PE14.7))
97 VTRY = VRIG2
99 XTRY = XRIG2
    WRITE(6,98)
98 FORMAT(18H ITERATION FAILURE)
104 IF((FCTN2(II-1).LT.FCTLIM).AND.(FCTN2(JJ+1).LT.FCTLIM)) GO TO 201
    IF(FCTN2(II-1) - FCTN2(JJ+1)) 106,108,108
108 IF(II.NE.2) GO TO 105
    CALL MOVRIG
    JJ = JRIGID + 2
    RETURN
105 II = II - 1
    X1SUM = X1SUM + X1(II)
    VISUM = VISUM + V1(II)
    GO TO 220
106 IF(JJ.NE.M-1) GO TO 107
    JJ = M
    RETURN
```

FAILING
FAILING
FAILING
FAILING
FAILING


```
107 JJ = JJ + 1
    X1SUM = X1SUM + X1(JJ)
    V1SUM = V1SUM + V1(JJ)
    GO TO 220
201 IF(II.EQ.2) GO TO 205
    DELL = DELLO - DELT*(FCTN2(II-1) + FCTN2(II-2))*0.5
    X2(II-1) = X2(II-2) + DELL
205 RIGID(II-1) = .FALSE.
    SIG(II-1) = DELM/(DELLO - DELT*FCTN2(II-1))
    F(II-1) = FO + KMROOT*(FCTN2(II-1) + FCTN1(II-1))*0.5
C   COMPUTE MASS DENSITY, DISPLACEMENT, VELOCITY, AND SPRING FORCE
C   FOR ALL RIGID SEGMENTS IN FLOATING RIGID BODY
    X2(II) = XRIG2 - DELMIN*FLOAT(JJ - II)/2.
    DO 224 I=II,JJ
        V2(I) = VRIG2
        X2(I) = X2(II) + FLOAT(I - II)*DELMIN
        FCTN2(I) = FCTMAX
        RIGID(I) = .TRUE.
        SIG(I) = SIGMAX
224 F(I) = F(I-1) - DMDT*(V2(I-1) + V2(I) - V1(I-1) - V1(I))*0.5
    IF(JJ.NE.M-1) GO TO 206
    JJ = M
    RETURN
206 DELL = DELLO - DELT*(FCTN2(JJ) + FCTN2(JJ+1))*0.5
    X2(JJ+1) = X2(JJ) + DELL
    RIGID(JJ+1) = .FALSE.
    SIG(JJ+1) = DELM/(DELLO - DELT*FCTN2(JJ+1))
    F(JJ+1) = FO + KMROOT*(FCTN2(JJ+1) + FCTN1(JJ+1))*0.5
    JJ = JJ + 2
    RETURN
END
```

```
SUBROUTINE FIXRIG(II)
COMMON DELT,DELT2,LINT,M,DELLO,X2(100)
LOGICAL RIGID
REAL KMROOT
COMMON /ONE/ RIGID(100),F(100),FCTN1(100),FCTN2(100),V1(100),
1 V2(100),X1(100),SIG(100),FCTLIM,FCTMAX,SIGMAX,DELMIN,DMDT,DELM,
2 KMROOT,FO,JRIGID,IRIGID
IRIGID = II
214 IF(IRIGID.LE.2) GO TO 215
    FCTN2(IRIGID-1) = ((1.5*DELLO - (X2(M) - DELMIN*(FLOAT(M - IRIGID)
1 + 0.5) - X2(IRIGID-2)))/DELT - FCTN2(IRIGID-2))*0.5
    IF(FCTN2(IRIGID-1).LE.FCTLIM) GO TO 216
    IRIGID = IRIGID - 1
    GO TO 214
```

```
215 FCTN2(1) = (DELLO - 2.*(X2(M) - DELMIN*(FLOAT(M-2) + 0.5) -  
1 X2(1)))/DELT  
IF(FCTN2(1).LE.FCTLIM) GO TO 218  
WRITE(6,200)  
200 FORMAT(/24H SPRING COMPRESSED SOLID)  
CALL EXIT  
216 V2(IRIGID-1) = FCTN1(IRIGID-2) + V1(IRIGID-2) - FCTN2(IRIGID-1)  
DELL = DELLO - DELT*(FCTN2(IRIGID-1) + FCTN2(IRIGID-2))*0.5  
X2(IRIGID-1) = X2(IRIGID-2) + DELL  
218 RIGID(IRIGID-1) = .FALSE.  
SIG(IRIGID-1) = DELM/(DELLO - DELT*FCTN2(IRIGID-1))  
F(IRIGID-1) = FO + KMROOT*(FCTN2(IRIGID-1) + FCTN1(IRIGID-1))*0.5  
C COMPUTE MASS DENSITY, DISPLACEMENT, VELOCITY, AND SPRING FORCE  
C FOR ALL RIGID SEGMENTS ATTACHED TO THE FIXED END  
DO 217 I=IRIGID,M  
V2(I) = 0.  
FCTN2(I) = FCTMAX  
RIGID(I) = .TRUE.  
SIG(I) = SIGMAX  
X2(I) = X2(M) - FLOAT(M - I)*DELMIN  
217 F(I) = F(I-1) - DMDT*(V2(I-1) - V1(I) - V1(I-1))*0.5  
RETURN  
END
```

DOCUMENT CONTROL DATA - R & D

(Security classification of title, body of abstract and indexing annotation must be entered when the overall report is classified)

1. ORIGINATING ACTIVITY (Corporate author)		2a. REPORT SECURITY CLASSIFICATION	
Iowa Institute of Hydraulic Research		Unclassified	
		2b. GROUP	
3. REPORT TITLE			
Motion of a helical spring due to dynamic loading			
4. DESCRIPTIVE NOTES (Type of report and, inclusive dates)			
Technical Report			
5. AUTHOR(S) (First name, middle initial, last name)			
David W. McDougall, and Enzo O. Macagno			
6. REPORT DATE		7a. TOTAL NO. OF PAGES	7b. NO. OF REFS
September 1968		56	4
8a. CONTRACT OR GRANT NO.		9a. ORIGINATOR'S REPORT NUMBER(S)	
b. PROJECT NO. DA-11-070-508-ORD-988		Report No. 112	
c.		9b. OTHER REPORT NO(S) (Any other numbers that may be assigned this report)	
d.			
10. DISTRIBUTION STATEMENT			
Each transmittal of this document outside the Department of Defense must have prior approval of the R. & E. Division, Rock Island Arsenal.			
11. SUPPLEMENTARY NOTES		12. SPONSORING MILITARY ACTIVITY	
		Rock Island Arsenal	
13. ABSTRACT			
<p>A one-dimensional model is presented which is suitable for describing the internal motions and force distribution of a helical spring that is subjected to dynamic loading. The accompanying analysis was carried out by digital computer. Elastic behavior was treated by the method of characteristics, and coil closure simulated and treated by rigid-body-motion equations. Satisfactory model verification was achieved by the analysis of high-speed motion pictures of a physical experiment. Descriptive flow charts of the computational technique and complete FORTRAN listings are included.</p>			

14. KEY WORDS	LINK A		LINK B		LINK C	
	ROLE	WT	ROLE	WT	ROLE	WT
Recoil Mechanism						
Shock Absorber						
Dynamic Spring						
Spring Transients						